AD-A256 483

(3)

PL-TR-92-2160

# RADIATION BELT DYNAMIC AND QUASI-STATIC MODELING BASED ON CRRES DATA: OUTER-BELT SHORT-TERM RESPONSE DATA BASE


Y. T. Chiu
M. A. Rinaldi
W. E. Francis
R. M. Robinson
R. W. Nightingale





Lockheed Palo Alto Research Laboratory
Space Sciences Laboratory 0/91-20, B/255
3251 Hanover Street
Palo Alto, CA 94304-1191



15 June 1992

Scientific Report No. 2





PHILLIPS LABORATORY
AIR FORCE SYSTEMS COMMAND
HANSCOM AIR FORCE BASE, MA 01731-5000

"This technical report has been reviewed and is approved for publication"

KEVIN J. KERNS, Capt, USAF
Contract Manager

E. G. MULLEN
Branch Chief

WILLIAM SWIDER
Deputy Director

This document has been reviewed by the ESD Public Affairs Office (PA) and is releasable to the National Technical Information Service (NTIS).

Qualified requestors may obtain additional copies from the Defense Technical Information Center. All others should apply to the National Technical Information Service.

If your address has changed, or if you wish to be removed from the mailing list, or if the addressee is no longer employed by your organization, please notify PL/TSI, Hanscom AFB, MA 01731. This will assist us in maintaining a current mailing list.

Do not return copies of this report unless contractual obligations or notices on a specific document requires that it be returned.

# REPORT DOCUMENTATION PAGE

Form Approved
OMB No. 0704-0188



**1. AGENCY USE ONLY** *(Leave blank)*

**2. REPORT DATE**
15 June 1992

**3. REPORT TYPE AND DATES COVERED**
Scientific Report No. 2

**4. TITLE AND SUBTITLE**
Radiation Belt Dynamic and Quasi-Static Modeling Based on CRRES Data: Outer-Belt Short-Term Response Data Base

**5. FUNDING NUMBERS**
PE 62101F
PR 7601 TA 22 WU LA

Contract F19628-90-C-0097

**6. AUTHOR(S)**
Y. T. Chiu
M. A. Rinaldi
W. E. Francis
R. M. Robinson
R. W. Nightingale

**7. PERFORMING ORGANIZATION NAME(S) AND ADDRESS(ES)**
Lockheed Palo Alto Research Laboratory
Space Sciences Laboratory 0/91-20, B/255
3251 Hanover Street
Palo Alto, CA 94304-1191

**8. PERFORMING ORGANIZATION REPORT NUMBER**

**9. SPONSORING/MONITORING AGENCY NAME(S) AND ADDRESS(ES)**
Phillips Laboratory
Hanscom AFB, MA 01731-50000

Contract Manager: Kevin Kerns, Capt, USAF/GPSP

**10. SPONSORING/MONITORING AGENCY REPORT NUMBER**
PL-TR-92-2160

**11. SUPPLEMENTARY NOTES**

**12a. DISTRIBUTION/AVAILABILITY STATEMENT**
Approved for public release; distribution unlimited

**12b. DISTRIBUTION CODE**

**13. ABSTRACT** *(Maximum 200 words)*
This report summarizes achievements made in the second year of the subject contract. New features of the outer radiation belt dynamic response to geomagnetic storms are characterized using CRRES data. The response is found to have an intermediate (10-20 days) time scale and an intense short time scale (1-2 days). The intermediate time scale changes are characterized as invariant-violating diffusion, as has been developed by us for SCATHA data. The short time scale decreases of flux are characterized as adiabatic (reversible) dynamics, conserving the first invariant under trapping volume change.

**14. SUBJECT TERMS**
Radiation belts
Geomagnetic storms
Radiation dose

**15. NUMBER OF PAGES**
44

**16. PRICE CODE**

| 17. SECURITY CLASSIFICATION OF REPORT | 18. SECURITY CLASSIFICATION OF THIS PAGE | 19. SECURITY CLASSIFICATION OF ABSTRACT | 20. LIMITATION OF ABSTRACT |
|---|---|---|---|
| Unclassified | Unclassified | Unclassified | SAR |

# CONTENTS

1. Introduction

This report summarizes scientific and technical activities in the period from June 15, 1991 to June 15, 1992. The chief activities in this period are the assembling of a modeling data base for the outer belt which includes the complete science data analysis for the outer electron belt and the collection of supplemental data such as Dst and Kp. While these data activities were taking place, we have not neglected the area of publication and presentation of interim results which turned out to be of interest to the radiation belt community, in both theoretical and observational developments in our program.

Exhibits of our scientific papers and samples of our outer belt electron modeling data base developed and completed in this contract period are presented here to document our scientific and technical achievements.

2. Data Base Development

During this year we have completed the science data analysis for the high energy electrons for the entire CRRES lifetime.

During the second quarter we have improved the capabilities to display the CRRES SEP database in terms of pitch-angle distributions. The final distributions are binned into 4 degree pitch-angle bins and 12 energy channels ranging from 405 keV to > 5 MeV. The SEP instrument regularly sees the loss cone both near 0 and 180 degrees, so that near-loss cone high-energy electrons studies may also be done. These distributions are also time averaged or binned into whole or fractional L shell bins. This will facilitate the comparison of pitch-angle distributions dynamics from electrons in the same L shell, but different MLT during the same orbit or over multiple orbits. Time averaged displays can also be used to see the evolution of a distribution during the different phases of a sudden commencement event. Using ephemeris data, we can also project the distributions to the magnetic equator where intercomparisons between data sets can be made. These comparisons will be used to study sudden commencements and the dynamics of the distributions during these events.

Long timescale, line-plot displays of the high energy (> 400 keV) electron database has shown many sudden commencement events on timescales of hours, days and sometimes weeks. The longer events are usually characteristic of major storms. The smaller events are characterized by short time scales and intense electron flux changes. These smaller events are interesting, in that, they allow us to study large electron-flux adiabatic changes in a relatively short-time interval (1 orbit). Comparison between sudden commencements and Dst shows a high degree of general correlation. The entire Dst data base finally arrived in May 1992. The magnetospheric compressions, inferred from these correlations, are usually adiabatic in that electron fluxes return to previous levels after the event. For a science discussion, see Section 3 and Exhibit 1 below. In several cases, we have seen the SEP instrument sample the same L shell at different magnetic local times within a single complete orbit. At times this type of sampling allows us to study the time evolution of a sudden commencement event. Studying the changes in the projected pitch-angle distribution functions have given us significant insight into the dynamic features of these events. We have now a solid observational base from which to begin our dynamic modeling of the magnetosphere.

The outer belt high energy electron modeling data base consists of two superposed segments such as that shown on Figure 1. The first segment is of intermediate time scale and is diffusive in signature. This data base is not different from what we have constructed for the SCATHA diffusion study. We have reduced the entire SEP data set so that all the outer belt electron data can be decomposed into eigenfunctions of diffusion. The code for simultaneous radial and pitch angle diffusion analysis of SCATHA/SEP data has been modified to suit the CRESS orbit, which allows for space-time separation in a much more distinct manner. In the new code, the time dependence will be determined by data directly in the diffusion fit, rather than through assumptions, as in the SCATHA/SEP analysis. Since we have published our completed work in this connection, we shall not belabor this part of data base construction here.

Because of the highly elliptical orbit of CRRES, the data base is suitable for short time scale analysis in a manner that allows for clear separation of space and time. The CRRES data show copious events of flux decreases in response to Dst changes. These events of 1-3 orders of magnitude in flux decrease over an event duration of 1-2 days constitute the major portion of outer belt electron responses to geomagnetic activity. An outer belt model cannot be complete without characterizing these features. We have collected a data base of 17 such events together with the corresponding highly-time resolved Dst and magnetic field records to form a Short Term Response data base, which is a unique feature of our CRRES dynamic modeling effort. All the details of the data for these 17 events have been analyzed and collated. The space-time parameters of the 17 short response events forming our quantitative modeling data base are summarized in the table in Figure 2. A sample of the individual event scenario as indicated by the distribution function for 3 of the 17 events is shown as Figures 3, 4, and 5. The scenario of rapid development and recovery to approximately the pre-event state of the outer belt is evident in these samples.

Several hypothesis for the physical explanation of these short term events have been examined cooperatively with Dr. Mike Schulz of the Aerospace Corporation. Only one of these, trapping volume increase by ring current reduction of the magnetic field, seems to be able to yield a rough quantitative account for the multiple properties of the short response data base. It now remains to be seen if this hypothesis can yield a quantitative model of the short term responses. For an exposition of the physical principles, the reader is referred to the next section and to Exhibit 1, which is a paper recently submitted to the Journal of Geophysical Research.

3. Science

A paper entitled "Dynamical Behavior of Outer-Belt Relativistic Electrons" by Y.T. Chiu and M.A. Rinaldi has been submitted for publication in the Journal of Geophysical Research.

This paper reports on the intermediate and short-term dynamical behavior of outerbelt relativistic electrons as seen by the Lockheed SEP instrument on board the CRRES mission. The high-energy electron distribution function data is organized for purposes of dynamic modeling to take advantage of the mission orbit to reveal features of outer belt dynamics not available to geosynchronous or other missions. The fluxes of outer belt electrons of energy greater than 400 keV were found to vary over two distinctly different characteristic time scales over the lifetime of CRRES: (1) an irregular fluctuation of an order of magnitude with a time scale of tens of days or longer, and (2) a geomagnetically related flux decrease and subsequent recovery of up to three orders of magnitude with a time scale of less than several days. Unlike the inner belt, the average levels of outer belt relativistic electrons over the long term are not substantially elevated by the historic storm of March 1991. Some primitive concepts of quantitative modeling for the short-term responses led to an understanding of these in terms of first adiabatic invariant conservation for the relativistic electron population.

Extensive discussions on the short term variations of outer belt electrons were held with Dr. Mike Schulz and several hypotheses were tested. None agreed with the data (see data base section) better than first adiabatic invariant conservation in a drastic increase of trapping volume. Details of the dynamical concept are discussed in the paper, the full text of which is submitted here as Exhibit 1 of the Annual Science and Technical Report. We shall not belabor the arguments here except to note that the total outer belt model that seems to fit involves a distribution function with two time-scale factors. One factor is a distribution that conserves the first invariant, so it is a function of the second and third invariant in a form approximately the same as that in the SCATHA diffusion model [Chiu et al., 1988, 1989, 1990]. The other factor, modeling the short term response is a power law of the first invariant. This model is quite consistent with both physics and data.

A second paper on outer magnetosphere modeling is near completion, pending inclusion of effects in the magnetotail region. Dr. Mike Schulz, co-author, has set up some

calculations to improve its magnetotail behavior. Bill Francis is currently implementing these. From the standpoint of outer belt dynamic modeling, the magnetotail behavior is not crucial. During this period, a joint paper with Aerospace entitled "Source Surface Model of the Magnetosheath" has been presented as an invited paper at the IAGA meeting at Vienna by Dr. Mike Schulz of Aerospace. The full paper for the Journal of Geophysical Research is being prepared. The front page is shown here as Exhibit 2.

4. Future Work

Implementation of the two-time-scale dynamical model of the outer belt relativistic electrons is of the highest priority in our program. All the computational ingredients are currently in place for application to the data base of the 17 short term events plus the longer term response background. Because of direct relation to first invariant conservation, the short-term factor of the distribution function will be characterized in invariant coordinates. The intermediate-term factor of the distribution function is diffusive and is a function of the second and third invariants. Here we have a choice of directly adopting the *SCATHA* diffusion model in configuration and energy coordinates or developing a newer invariant coordinate description. At this point, the invariant coordinate description seems to be viable because only 2-dimensional diffusion is necessary. However, the question of interpretation from abstract invariant space diffusion to physical simultaneous radial-pitch angle diffusion [Chiu et al., 1988, 1989, 1990] needs to be dealt with. We expect this will occupy the major portion of the next year, after which we will have a viable dynamical high energy electron model.

The second item that needs modeling treatment is the behavior of the outer belt electrons and ions in the severe environment of the March 1989 event. Investigation of this item next year will yield insights into the origin of the severe long-lived increases of radiation in the inner belt as well as the newly created inner relativisitc electron belt as our data analysis already indicated that the large fluxes of outer belt electrons due to the storm did not persist beyond the intermediate time scale of tens of days.

The third question that needs investigation is the nature of the physical processes that increase the trapping volume. Although the development of the ring current, reducing the magnetospheric field may account for most of the trapping volume increase, the quantitative data may require an even larger increase in trapping volume. If so, we need to return to the investigation of first-invariant conserving scattering of electrons with magnetospheric structures that we introduced into the physical infrastructure while awaiting the arrival and processing of CRRES/SEP data. We estimate that we will face this decision point at the latter part of next year, when our outer magnetosphere will have been complete.

## Figure Captions

Figure 1: Electron fluxes at two energy channels averaged over the L-value range shown. A highly-resolved trace of Dst is also shown for detailed comparison. Vertical time markers are also provided for convenience.

Figure 2: Space-time parameters of 17 short response events selected for our quantitative modeling data base.

Figure 3: Sample event of short response in Days 234-236 of 1990. (a) Dst history for the event, (b) space-time-Dst matrix of pitch angle distributions for Days 234-235, and (c) similar to (b) but for Days 235-236.

Figure 4: Sample event of short response in Days 254-256 of 1990: (a) Dst history for the event, (b) space-time-Dst matrix of pitch angle distributions for Days 254-255, and (c) similar to (b) but for Days 255-256.

Figure 5: Sample event of short response in Days 133-135 of 1991: (a) Dst history for the event, (b) space-time-Dst matrix of pitch angle distributions for Days 135-136, and (d) similar to (b) but for the remainder of Days 135.

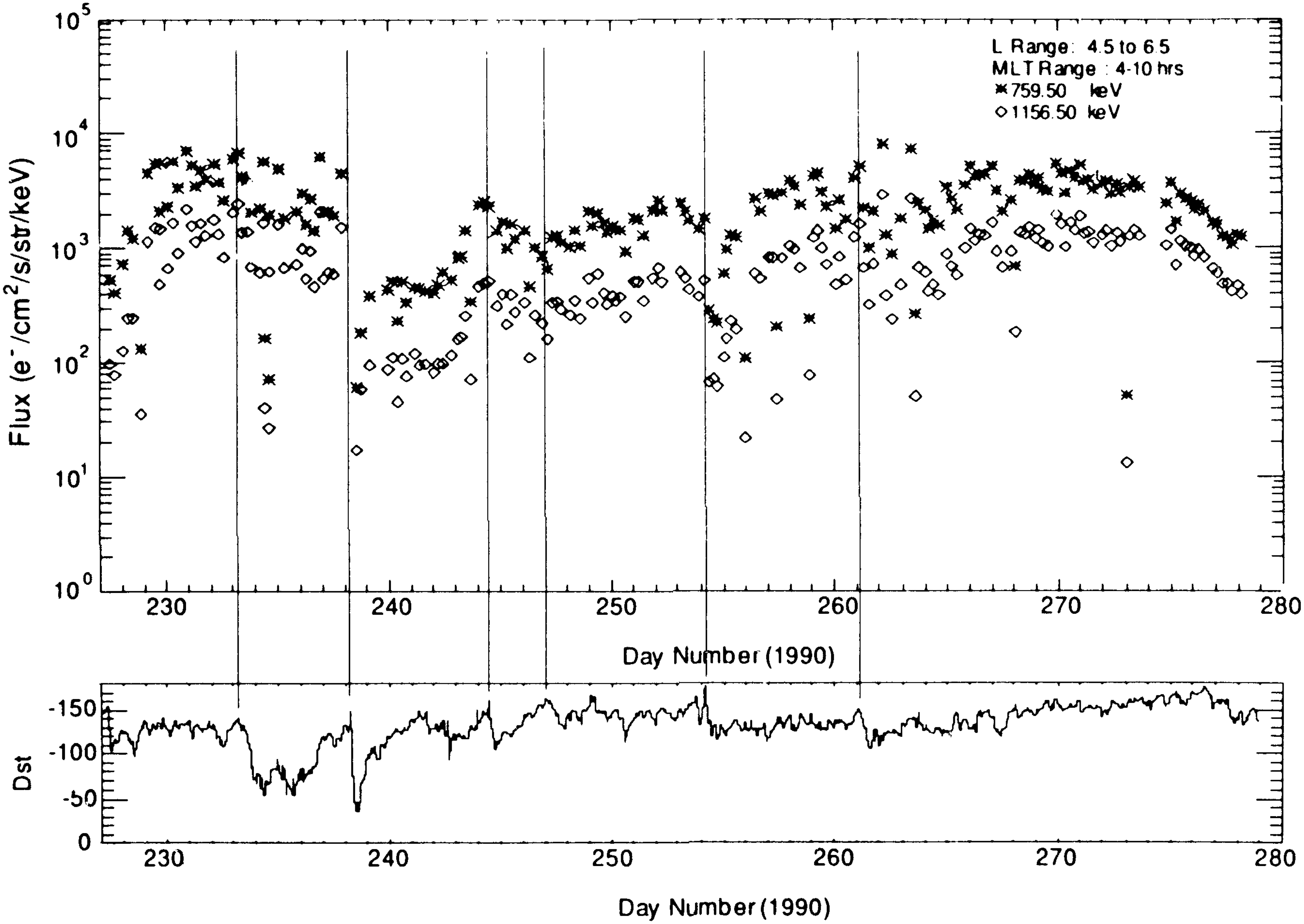
L Range: 4.5 to 6.5
MLT Range : 4-10 hrs
759.50 keV
1156.50 keV
Flux (e⁻/cm²/s/str/keV)
Day Number (1990)
Dst
Day Number (1990)

Figure 1

| Event No. | Day Number Range | Orbit Range | MLT | $L_{max}$ |
|---|---|---|---|---|
| 1 | 233-236 | 65-71 | 7 | 7.38 |
| 2 | 253-256 | 114-119 | 6.5 | 7.82 |
| 3 | 261-263 | 133-138 | 6 | 7.97 |
| 4 | 282-285 | 185-191 | 5.5 | 8.39 |
| 5 | 302-305 | 233-240 | 5 | 8.71 |
| 6 | 312-315 | 257-265 | 5 | 8.6 |
| 7 | 319-322 | 274-281 | 4.5 | 8.65 |
| 8 | 330-334 | 301-308 | 4 | 8.6 |
| 9 | 346-348 | 340-344 | 3.5 | 8.27 |
| 10 | 32-35 | 464-47[illegible] | 1 | 7.04 |
| 11 | 80-83 | 581-586 | 23 | 7.14 |
| 12 | 114-116 | 664-668 | 22 | 8.00 |
| 13 | 129-131 | 701-706 | 21.5 | 8.19 |
| 14 | 133-136 | 710-716 | 21.5 | 8.12 |
| 15 | 137-139 | 720-725 | 21 | 8.27 |
| 16 | 164-166 | 784-790 | 20 | 8.33 |
| 17 | 268-271 | 1027-1034 | 14 | 6.63 |
| 18 | 274-277 | 1043-1049 | 13.5 | 6.69 |

Figure 2

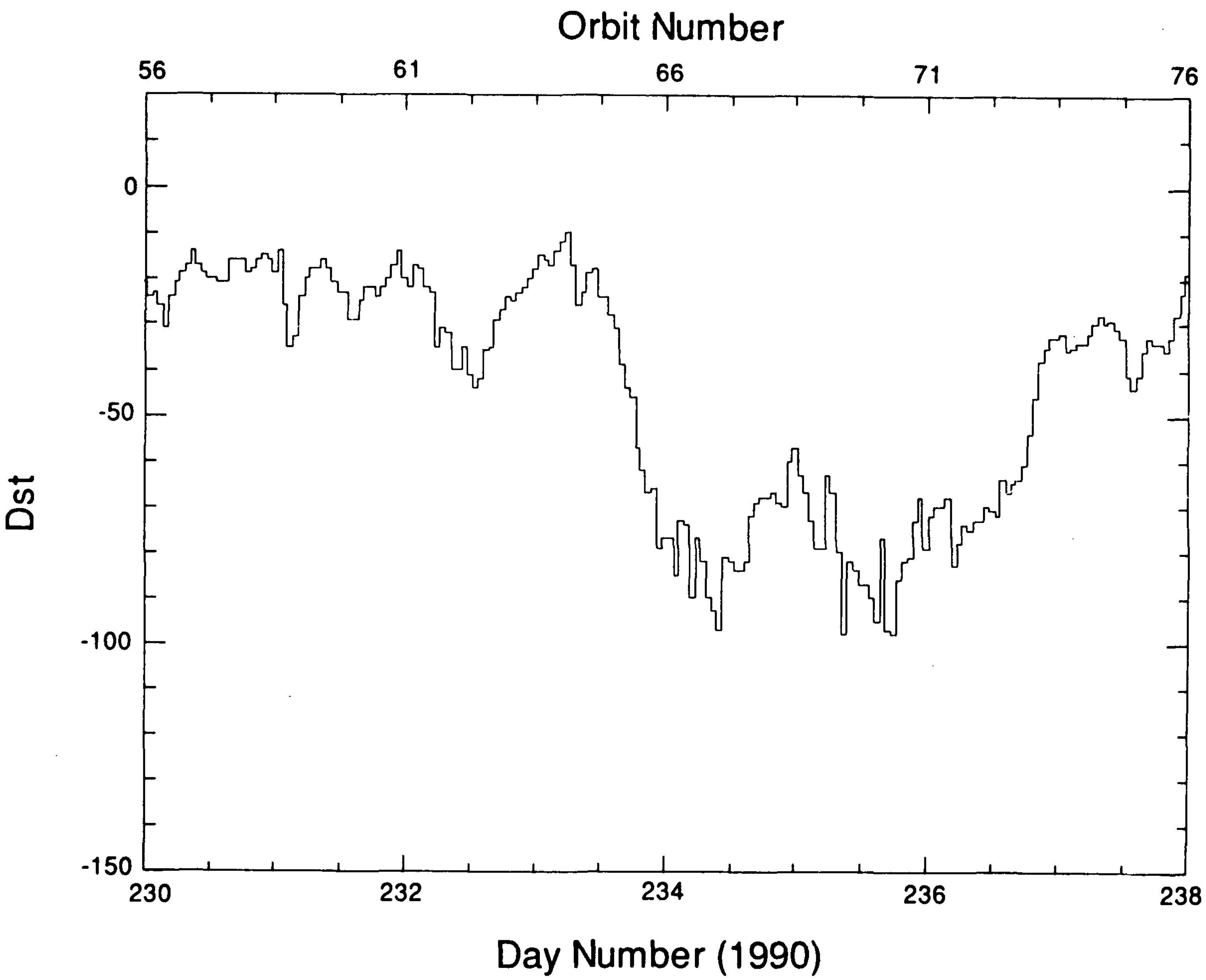
Orbit Number
56
61
66
71
76
0
-50
-100
-150
Dst
230
232
234
236
238
Day Number (1990)

Figure 3(a)

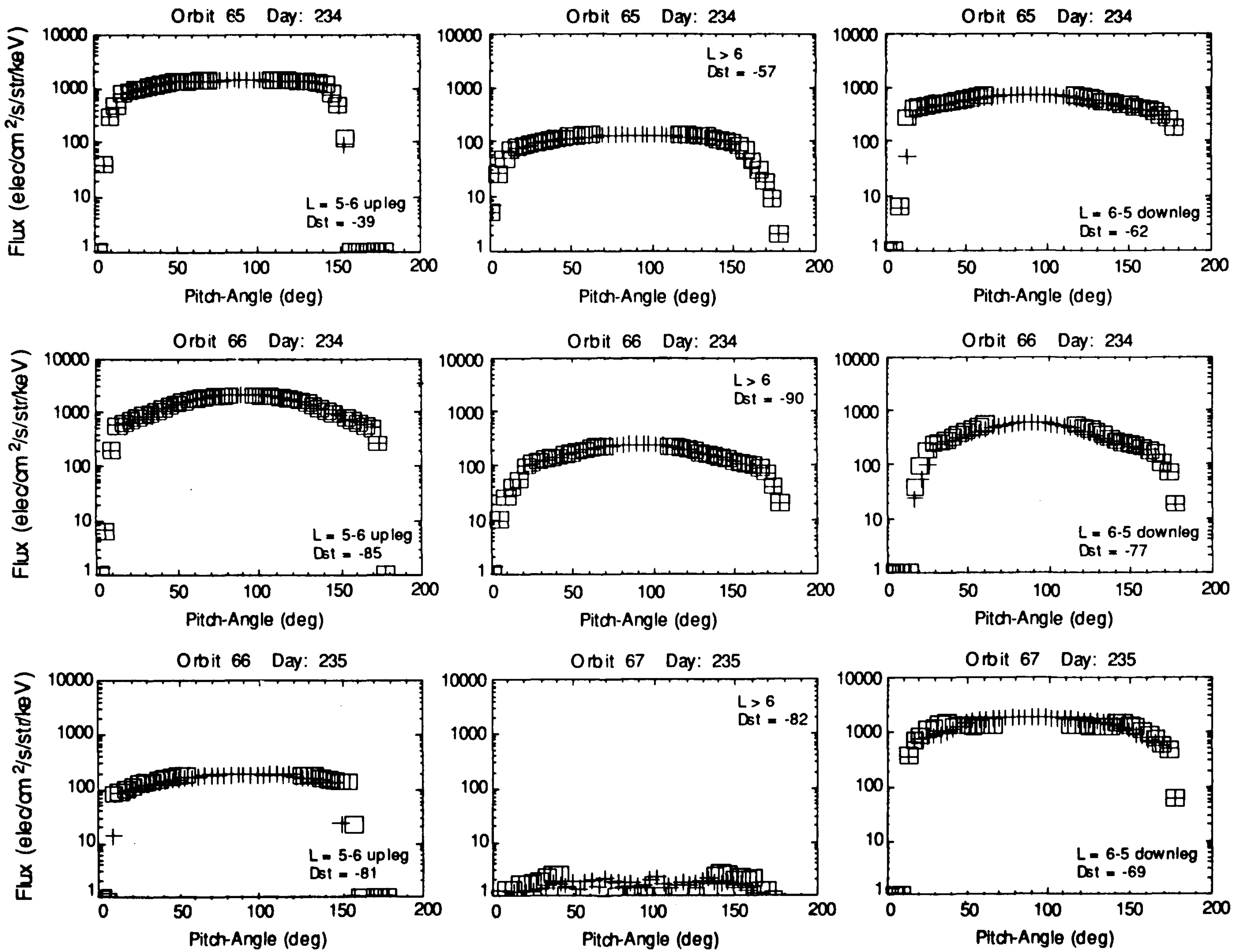
Orbit 65 Day: 234
L = 5-6 upleg
Dst = -39
Orbit 65 Day: 234
L > 6
Dst = -57
Orbit 65 Day: 234
L = 6-5 downleg
Dst = -62
Orbit 66 Day: 234
L = 5-6 upleg
Dst = -85
Orbit 66 Day: 234
L > 6
Dst = -90
Orbit 66 Day: 234
L = 6-5 downleg
Dst = -77
Orbit 66 Day: 235
L = 5-6 upleg
Dst = -81
Orbit 67 Day: 235
L > 6
Dst = -82
Orbit 67 Day: 235
L = 6-5 downleg
Dst = -69
Flux (elec/cm 2/s/str/keV)
Pitch-Angle (deg)

Figure 3(b)

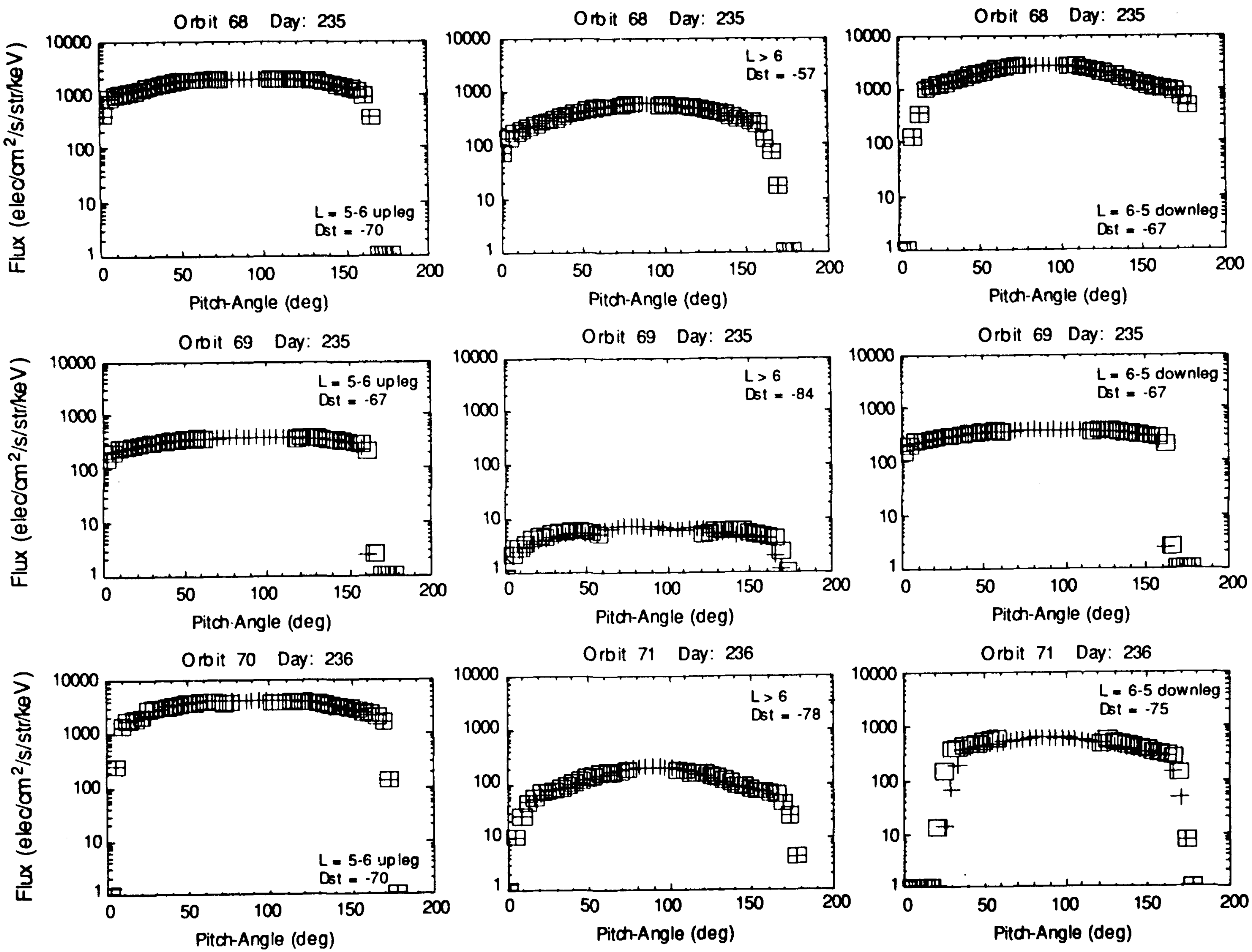

Orbit 68 Day: 235
L = 5-6 upleg
Dst = -70
Orbit 68 Day: 235
L > 6
Dst = -57
Orbit 68 Day: 235
L = 6-5 downleg
Dst = -67
Orbit 69 Day: 235
L = 5-6 upleg
Dst = -67
Orbit 69 Day: 235
L > 6
Dst = -84
Orbit 69 Day: 235
L = 6-5 downleg
Dst = -67
Orbit 70 Day: 236
L = 5-6 upleg
Dst = -70
Orbit 71 Day: 236
L > 6
Dst = -78
Orbit 71 Day: 236
L = 6-5 downleg
Dst = -75
Flux (elec/cm2/s/str/keV)
Pitch-Angle (deg)


Figure 3(c)

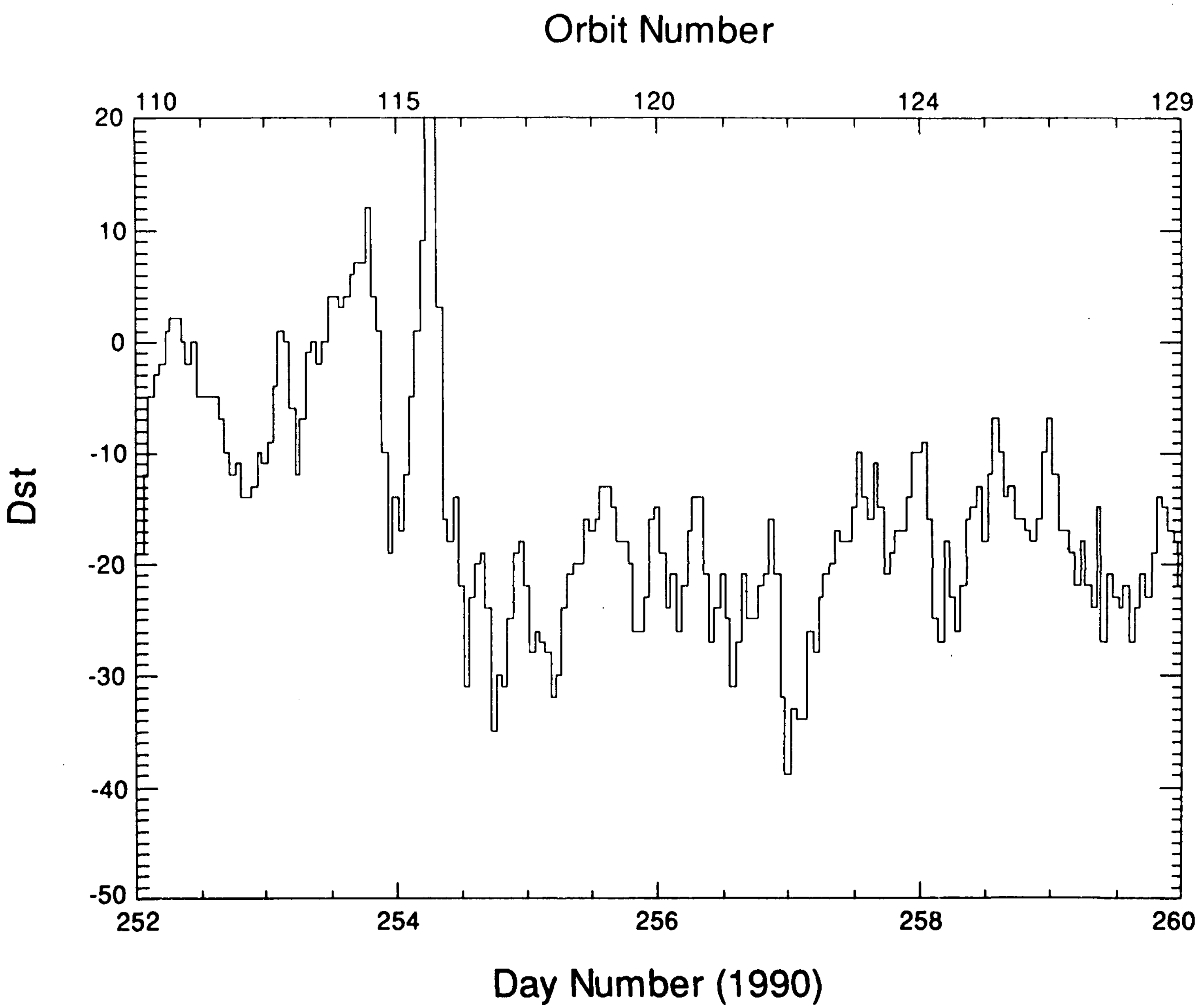
Orbit Number
110
115
120
124
129
20
10
0
-10
-20
-30
-40
-50
Dst
252
254
256
258
260
Day Number (1990)

Figure 4(a)

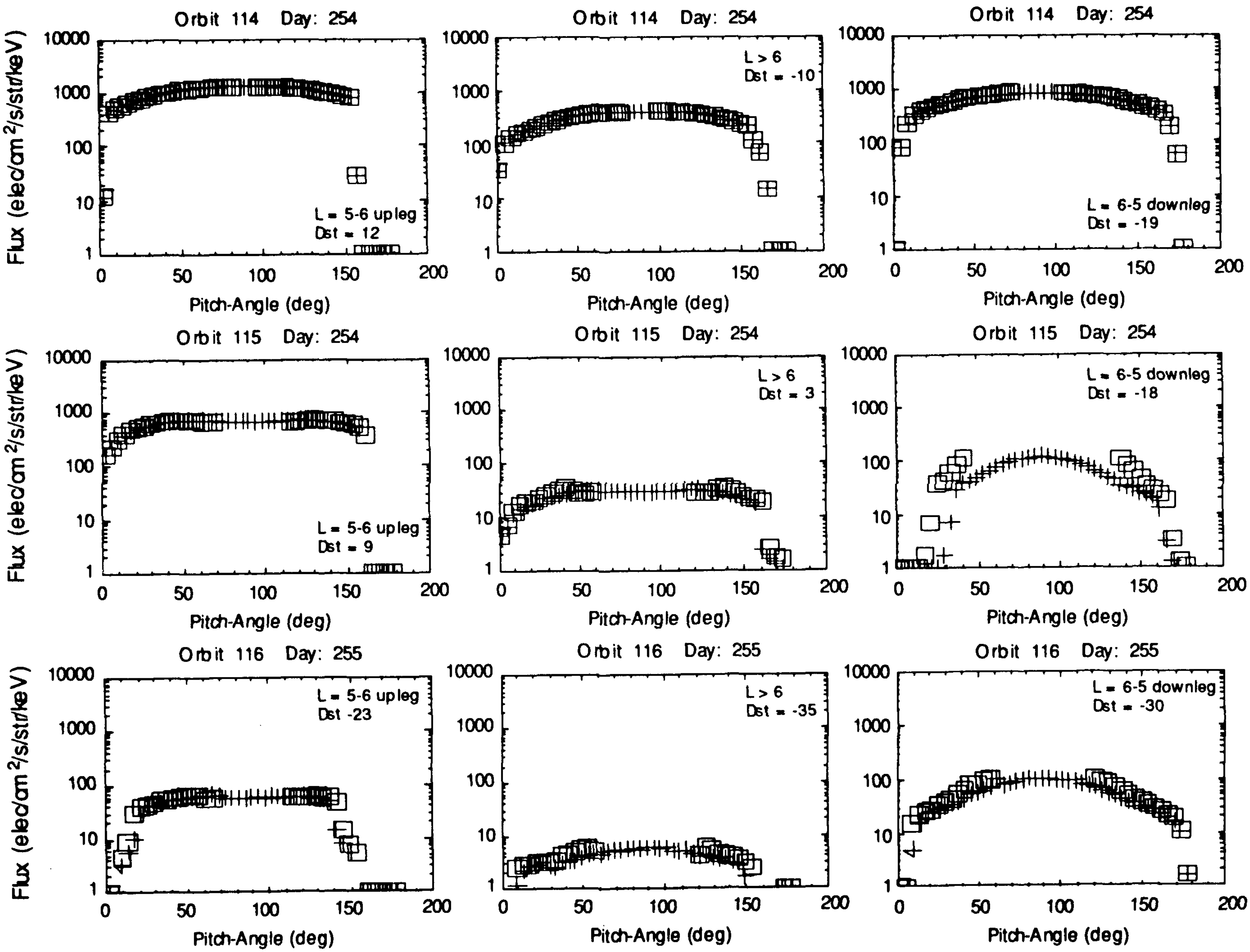
Orbit 114 Day: 254
L = 5-6 upleg
Dst = 12
Orbit 114 Day: 254
L > 6
Dst = -10
Orbit 114 Day: 254
L = 6-5 downleg
Dst = -19
Orbit 115 Day: 254
L = 5-6 upleg
Dst = 9
Orbit 115 Day: 254
L > 6
Dst = 3
Orbit 115 Day: 254
L = 6-5 downleg
Dst = -18
Orbit 116 Day: 255
L = 5-6 upleg
Dst -23
Orbit 116 Day: 255
L > 6
Dst = -35
Orbit 116 Day: 255
L = 6-5 downleg
Dst = -30
Flux (elec/cm 2/s/str/keV)
Pitch-Angle (deg)

Figure 4(b)

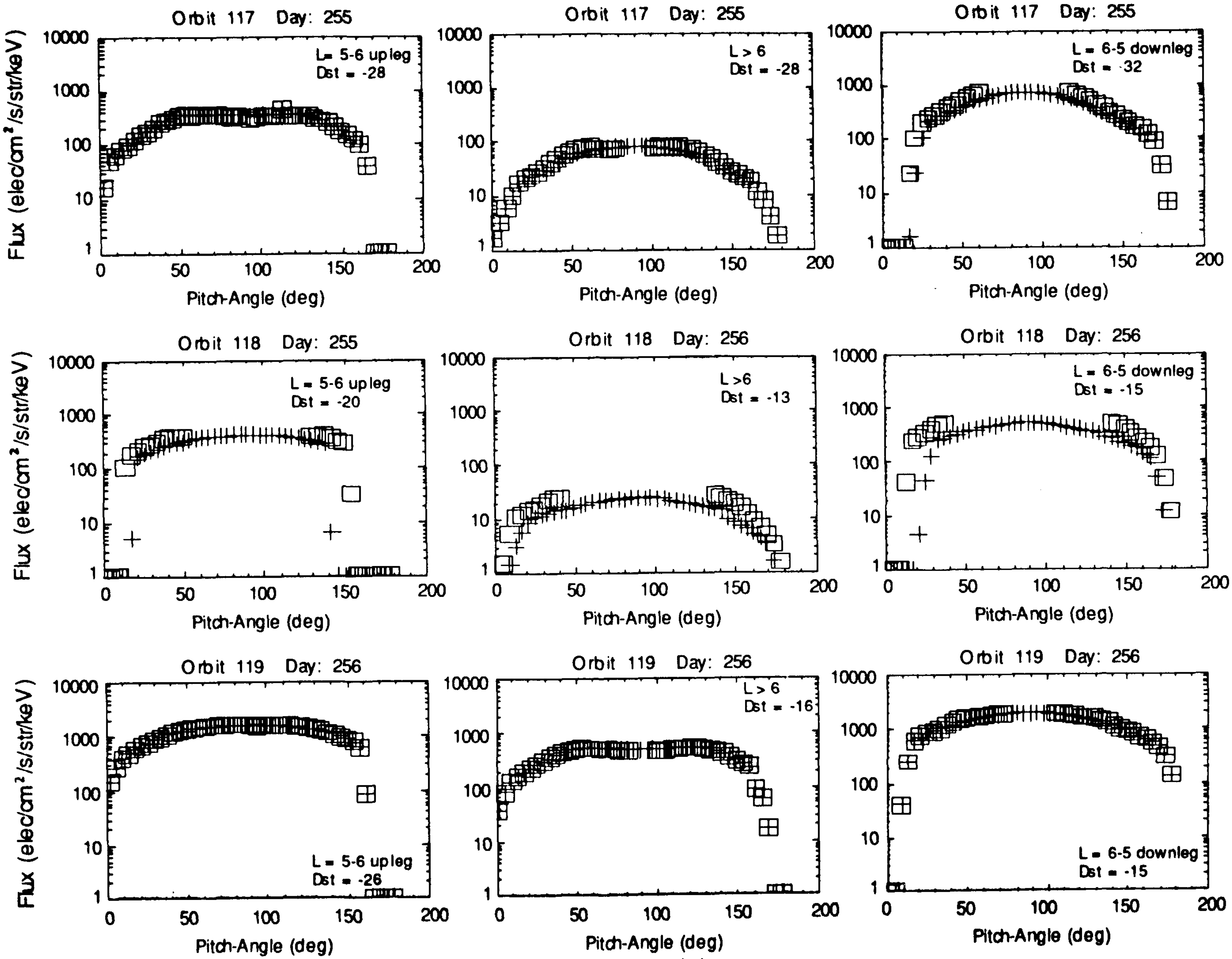
Orbit 117 Day: 255
L= 5-6 upleg
Dst = -28
L > 6
Dst = -28
L = 6-5 downleg
Dst = -32
Orbit 118 Day: 255
L = 5-6 upleg
Dst = -20
Orbit 118 Day: 256
L >6
Dst = -13
L = 6-5 downleg
Dst = -15
Orbit 119 Day: 256
L = 5-6 upleg
Dst = -26
L > 6
Dst = -16
L = 6-5 downleg
Dst = -15
Flux (elec/cm²/s/str/keV)
Pitch-Angle (deg)
10000
1000
100
10
1
0
50
100
150
200

Figure 4(c)

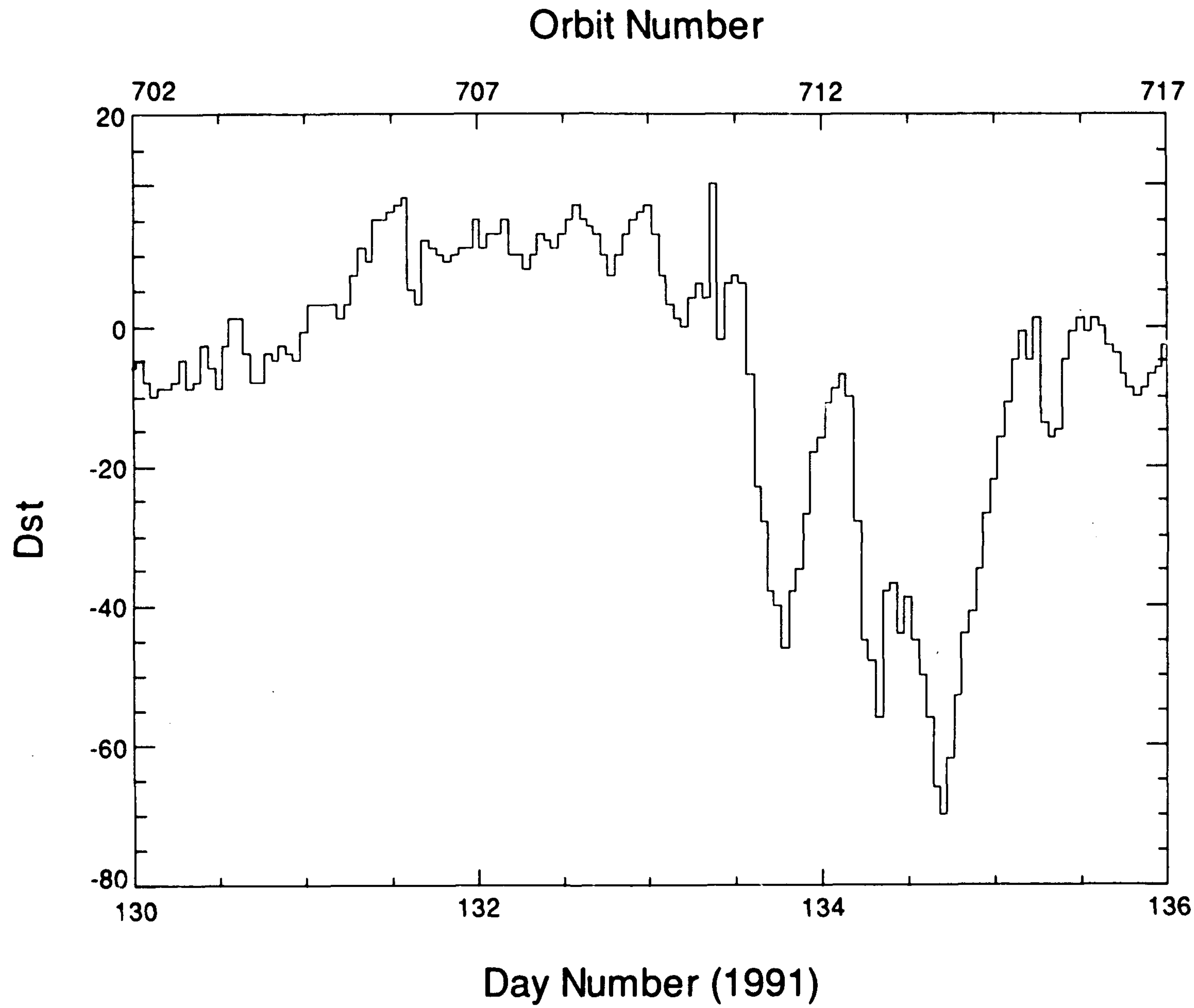
Orbit Number
702
707
712
717
20
0
-20
-40
-60
-80
Dst
130
132
134
136
Day Number (1991)

Figure 5(a)

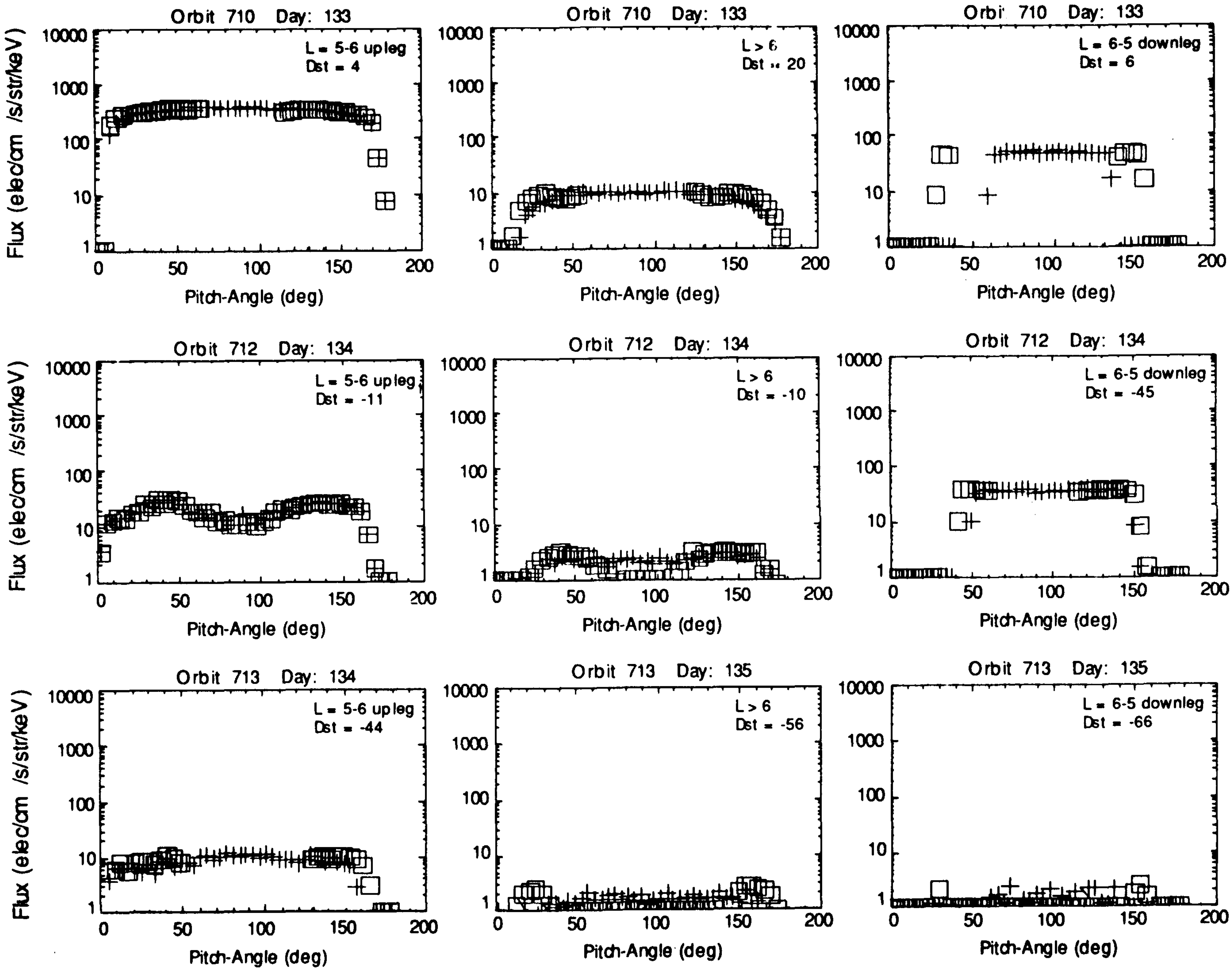
Orbit 710 Day: 133
L = 5-6 upleg
Dst = 4
Orbit 710 Day: 133
L > 6
Dst = 20
Orbit 710 Day: 133
L = 6-5 downleg
Dst = 6
Orbit 712 Day: 134
L = 5-6 upleg
Dst = -11
Orbit 712 Day: 134
L > 6
Dst = -10
Orbit 712 Day: 134
L = 6-5 downleg
Dst = -45
Orbit 713 Day: 134
L = 5-6 upleg
Dst = -44
Orbit 713 Day: 135
L > 6
Dst = -56
Orbit 713 Day: 135
L = 6-5 downleg
Dst = -66
Flux (elec/cm /s/str/keV)
Pitch-Angle (deg)

Figure 5(b)

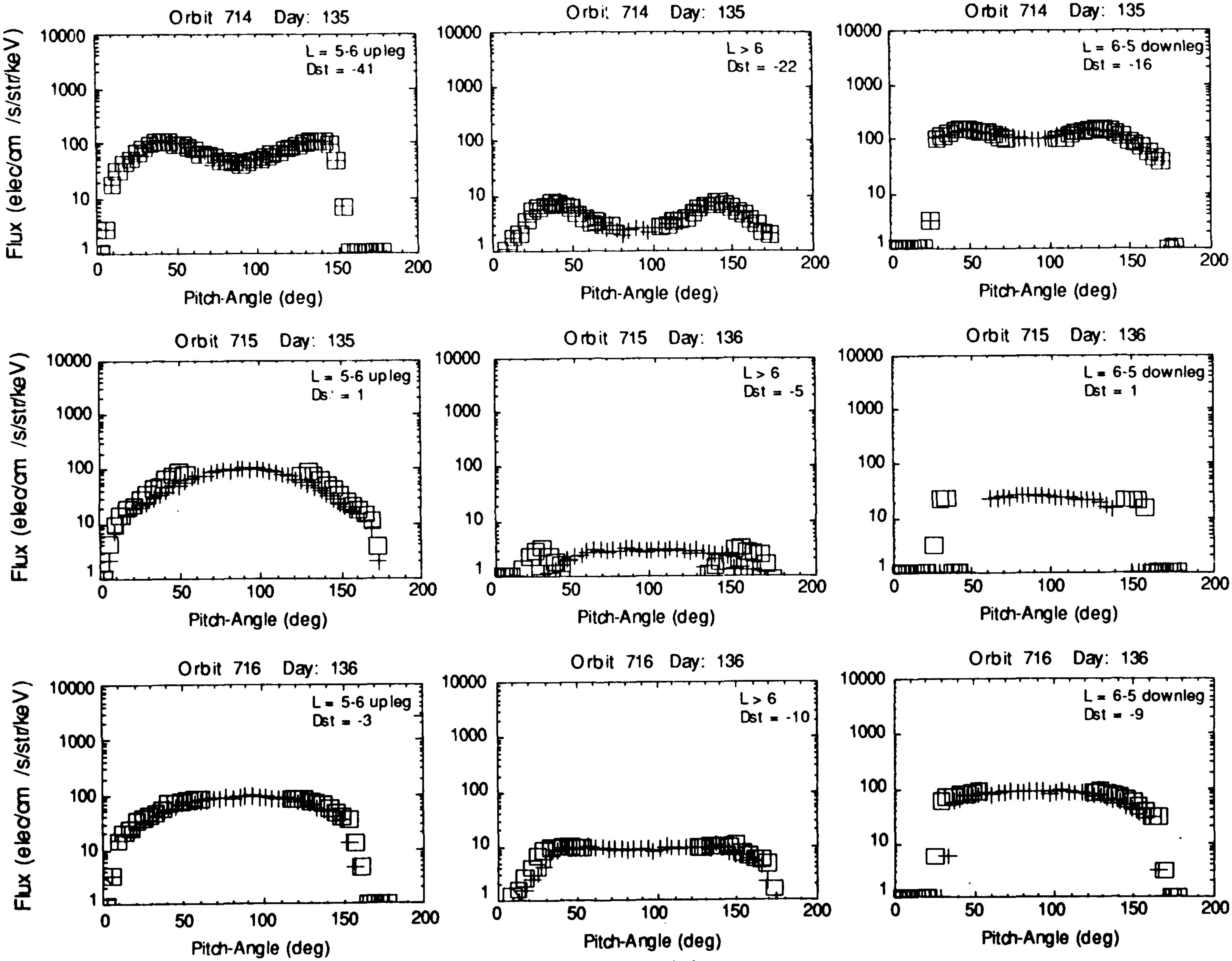
Orbit 714 Day: 135
L = 5-6 upleg
Dst = -41
Orbit 714 Day: 135
L > 6
Dst = -22
Orbit 714 Day: 135
L = 6-5 downleg
Dst = -16
Orbit 715 Day: 135
L = 5-6 upleg
Dst = 1
Orbit 715 Day: 136
L > 6
Dst = -5
Orbit 715 Day: 136
L = 6-5 downleg
Dst = 1
Orbit 716 Day: 136
L = 5-6 upleg
Dst = -3
Orbit 716 Day: 136
L > 6
Dst = -10
Orbit 716 Day: 136
L = 6-5 downleg
Dst = -9
Flux (elec/cm /s/str/keV)
Pitch-Angle (deg)

Figure 5(c)

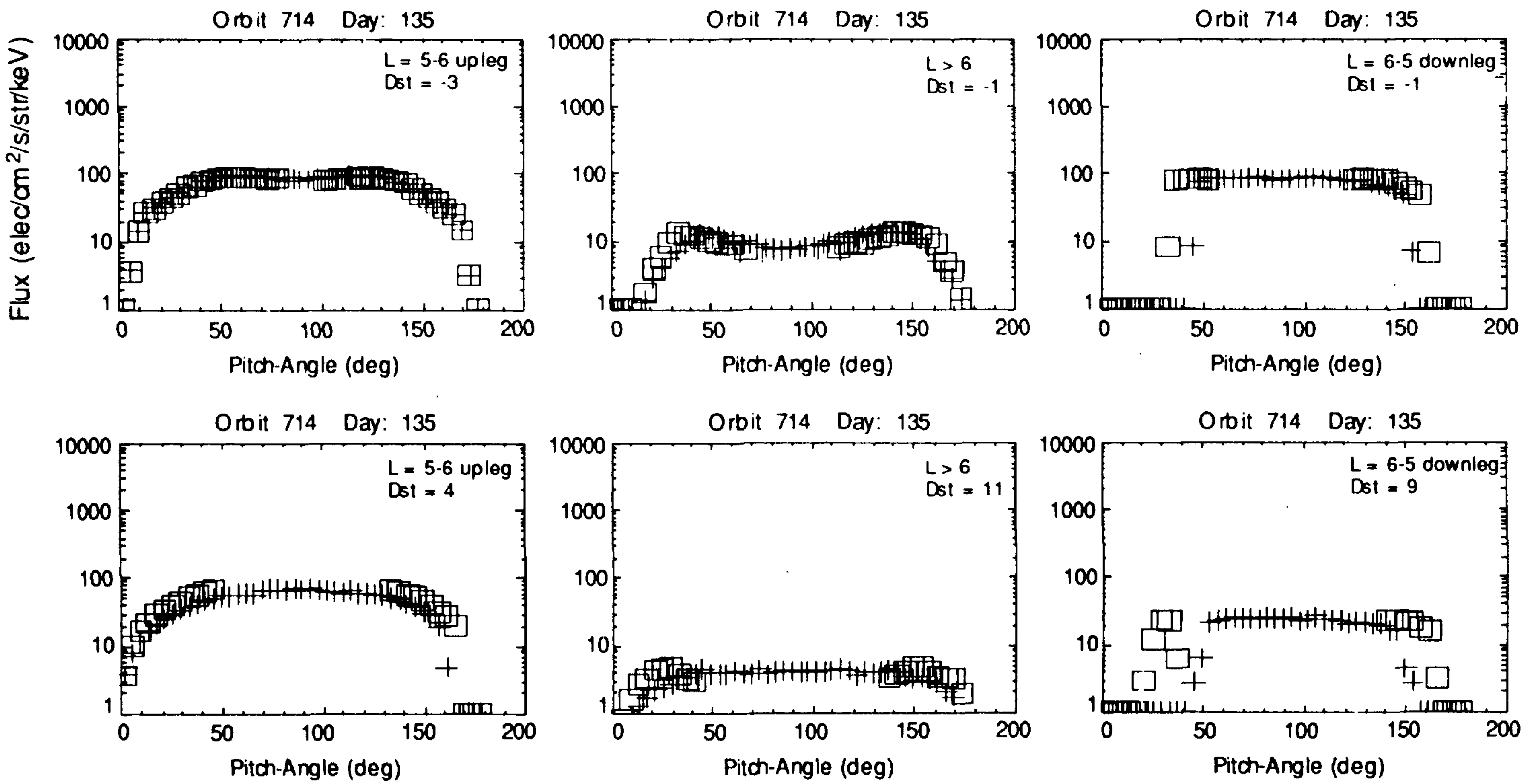
Orbit 714 Day: 135
L = 5-6 upleg
Dst = -3
Orbit 714 Day: 135
L > 6
Dst = -1
Orbit 714 Day: 135
L = 6-5 downleg
Dst = -1
Orbit 714 Day: 135
L = 5-6 upleg
Dst = 4
Orbit 714 Day: 135
L > 6
Dst = 11
Orbit 714 Day: 135
L = 6-5 downleg
Dst = 9
Flux (elec/cm²/s/s/str/keV)
Pitch-Angle (deg)
10000
1000
100
10
1
0
50
100
150
200

Figure 5(d)

EXHIBIT 1

# DYNAMICAL BEHAVIOR OF OUTER-BELT RELATIVISTIC ELECTRONS

Y.T. Chiu and M.A. Rinaldi

Lockheed Palo Alto Research Laboratory

3251 Hanover Street, Palo Alto, CA

## ABSTRACT

This paper reports on the intermediate and short-term dynamical behavior of outer-belt relativistic electrons as seen by the Lockheed SEP instrument on board the CRRES mission. The high-energy electron distribution function data is organized for purposes of dynamic modeling to take advantage of the mission orbit to reveal features of outer belt dynamics not available to geosynchronous or other missions. The fluxes of outer belt electrons of energy higher than 400 keV were found to vary over two distinctly different characteristic time sacles over the lifetime of CRRES: (1) an irregular fluctuation of an order of magnitude with a time scale of tens of days or longer, and (2) a geomagnetically related flux decrease and subsequent recovery of up to three orders of magnitude with a time scale of less than several days. Unlike the inner belt, the average levels of outer belt relativistic electrons over the long term are not substantially elevated by the historic storm of March 1991. Some primitive concepts of quantitative modeling for the short-term responses led to an understanding of these in terms of first adiabatic invariant conservation for the relativistic electron population.

## INTRODUCTION AND DATA

The space radiation (SPACERAD) segment of the USAF/NASA Combined Release and Radiation Effects Satellite (CRRES) mission was launched into a geosynchronous transfer orbit for the purpose of making focused observations of the radiation belts. [Mullen and Gussenhoven, 1992; see also collection of CRRES papers in IEEE Transactions Nucl. Sci. 38, no. 6, December 1991 and in J. Spacecraft Rock., in press 1992]. With a complement of modern instruments, one of the scientific objectives of CRRES is to elucidate the dynamics of the high-energy electrons in the outer radiation belt. This paper reports on a characterization of the dynamical behavior of the relativistic energy electrons ($\geq$ 400 keV) in the outer belt (L$\sim$4–6.5), based on data collected by the ONR-307 Spectrometer for Electrons and Protons (SEP) on board CRRES/SPACERAD [Nightingale et al., 1992]. By appropriate space-time analysis of the outer belt relativistic electron distribution functions, uniquely available to CRRES because of its orbital geometry and instrumentation, we are able to give a succinct summary of the response time scales of these outer belt

electrons. The characterizations reported in this paper offer valuable additions to those outer belt characteriatics found in comparable data sets of geosynchronous [e.g. Baker et al.; 1978; 1990; and references therein], quasi-geosynchronous [e.g. Reagan et al., 1987, Chiu et al., 1988; 1990, and references therein] and other [e.g. Sibeck et al. 1987; West et al., 1981, Brown et al., 1968] satellites. The distinct advantage of the SEP/CRRES data is that we are able to determine the electron distribution functions as the response to geomegnetic activity progresses.

The data base for this paper consists of all electron distribution functions of energy channels above 400 keV in the nominal range L=4–6.5, although flux levels for channels above 2 MeV are too low to be of much statistical significance for construction of distribution functions. We excluded electrons of energy below 400 keV from consideration in this paper. The exclusion is solely for the purpose of simplifying the characterization tasks; indeed, the lower energy particles have historically been better monitored than the relativistic electrons.

## INTERMEDIATE-TERM VARIATIONS

In this section we characterize the behavior of outer belt relativistic electrons over a time scale comparable to the lifetime of CRRES, which is approximately 1 year. For this purpose, we display the behavior of such electron fluxes integrated over given L-value ranges and over pitch angles for given energy channels, both over a relatively long timeline (approximately over the first half of 1991) and over a shorter period showing more details of the integrated flux flunctuations in response to geomagnetic activity (approximately over 60 days in the latter part of 1990).

Figure 1 shows the flux of relativistic electrons in the $759.5 \pm 206.5$ keV energy channel integrated over all pitch angles and over the nominal L-value range of 5.5-6.5 for the indicated period. The L-value interval is usually within $\Delta L = 1$ of CRRES apogee and is usually on the outer portion of the trapped outer radiation belt. The magnetic local times sampled range continuously from ~3 MLT through midnight to ~15 MLT. The flux fluctuations exhibited in Figure 1, over several orders of magnitude, are in genreal agreement with characteristics of previous observations [Brown et al., 1968; Baker et al.1978, 1990; West et al., 1981; Siebeck et al., 1987; Reagan et al., 1989]. They consist of : (1) deep flux decreases of up to 3 orders of magnitude over time scales of ~1-2 days in response to geomagnetic activity as indicated here by the Kp index; (2) roughly one order of magnitude flux fluctuations over time scales of ~20 days without any obvious correlation with geomagnetic activity, although these may be related to solar rotation [Baker et al., 1990]; and (3) unlike the inner belt, intense geomagnetic storms, such as the historical

disturbance of March 1991, do not produce long-lasting electron flux increases in the outer belt beyond the ~20 day time scale of item (2) above.

The focus of this report is on the short-term responses and these will be considered in detail below. As for the intermediate-term flux fluctuations in our data base, we note in Figure 1 that the short-term responses are clearly superposed on them. We hypothesize that they are independent of origin and will be treated independently until our data show otherwise. From the physical point of view, the two time scales must also be of rather independent physical processes. In previous work [Chiu et al., 1988, 1990], we showed that electron flux changes at these intermediate time scales are consistent with diffusion time scales of both radial and pitch-angle processes, given initiations of whatever cause, e.g. from extra-magnetospheric injections [Baker et al., 1990]. Until quantitative work on our CRRES data base shows otherwise, there is little reason to assume at present that the intermediate-term fluctuations of Figure 1 require a very different explanation than diffusion physics used to interpret the SCATHA data previously. The question of sources of these fluctuations is an interesting one; unfortunately, the short lifetime of CRRES may not yield a sufficiently large data base to address this question with high statistics. These matters will be treated in due course in our analysis program.

## SHORT-TERM RESPONSES

Clearly Figure 1 can be viewed as a compressed survey of part of the data base. To afford a more detailed examination of the outer belt relativistic electron characteristics over similar time scales, Figure 2 shows pitch angle integrated fluxes over the major part of the outer belt (L range of 4.5-6.5) in the latter part of 1990. Unlike Figure 1, this L-range encompasses even more of the outer belt. While the general time responses shown on Figure 2 confirm that of Figure 1 even though the local times are different, four aspects of Figure 2 need to be noted. since they may impact physical interpretations.

First, the short-term flux responses are always decreases. This can only be accounted for by two possibilities: either transport in the velocity part of phase space, reducing the population in the indicated energy channel by selective acceleration to other energy channels, or transport in the configuration part of phase space, removing flux to a different location or increasing the trapping volume. The possibility of both processes occuring simultaneously remains open, of course.

Second, fluxes from two neighboring energy channels, $759.5 \pm 206.5$ keV and $1156.6 \pm 206.5$ keV, are shown in Figure 2. The fluxes of both channels respond in concert both in time and in flux intensity, maintaining an essentially constant flux offset factor even though the fluxes fluctuate up to 3 orders of magnitude over ~1-2 days. We have examined the

energy spectra over some sample periods and found that these short period responses involve little or no change in spectral shape, at least within the energy range above 400 keV and below 2 Mev. In other words, flux decreases in one energy channel is not due to bulk transport (by accleration or deceleration) in aggregate into another energy channel within the energy range, although this statement does not say that no acceleration or deceleration takes place on the individual particle level. It must be noted that this approximate "conservation" of spectral shape applies to short-term low-Dst responses only. Major storms such as the March 1991 event change the spectrum drastically.

Third, to emphasize correlation with geomagnetic activity, we display in Figure 2 the corresponding Dst index at high time resolution. The high degree of correlation between the short-time response events with Dst events is apparent on an event-by-event basis. However, the initiation times of an outer-belt relativistic electron response and that of a Dst event bear further scrutiny since they do not always appear to be coincident when examined at shorter time scales. For this purpose, vertical time lines are shown in Figure 2 as guides for the reader. This matter will be dealt with further in the next section.

Fourth, the short-term flux responses in Figure 2 tend to recover, at least for the simple Dst events, to the flux level just before initiation of the response of ~1-2 days duration. A statistical examination of this feature over the entire CRRES lifetime is required to quantify the degree of flux conservation before and after the responses ; however, examination by eye of Figures 1 and 2 shows that there is no *significant change* in the total flux before and after the event, certainly not comparable in any way to the flux decreases in the event itself.

These curious features of the short-term responses of the outer belt relativistic electrons clearly require detailed examination. Because of the orbit geometry, with apogee (L~6.5) located at the outer edge of the outer belt, CRRES affords a time-resolved sampling of the same L interval in the outer belt on the upleg as well as on the downleg within a short time of each other. Given a highly time-resolved Dst record and assuming no magnetic local time (MLT) dependence within about 2-3 hours, we can examine the question of initiation of the short-term responses of the outer belt relativistic electrons. Figures 3,4, and 5 show a sequence of the 759 keV channel distribution function data over intervals arranged in alphabetic order from A to R, covering three consecutive visits of CRRES to the apogee in Days 233-235 in 1990, as indicated by the orbit diagrams and the time markings on the Dst traces. The pitch angle distributions corresponding to space-time locations of the alphabetic measurements are also shown in these figures. From the Dst trace on Figure 3, the initiation of the Dst event seems complex when resolved to hourly averages; however, a Dst decrease seems to begin at ~3 UT on Day 233 (location D).

Examination of the pitch angle distributions and flux levels of Figures 3 and 4 shows that normal outer belt conditions were encountered throughout space-time locations A through G, which is at 10 UT on Day 234. A decrease is seen at H (11 UT on Day 234) but the severe flux drop of 2 orders of magntidue does not occur until location I (12 UT on Day 234). Comparing the apogee fluxes of C (Day 233) on Figure 3 with I (Day 234) on Figure 4 gives us a measure of the effect of Dst on fluxes at the same spatial point before and after the flux drop. Because measurements at G and H (Figure 4) do not show marked effects of flux drop, we conclude that either (a) the flux drop is a temporal effect occuring at H-K (11-15 UT Day 234); or (b) the flux drop is a spatial feature sitting at H-K after the last CRRES visit to the same L-value locations (E at ~5 UT Day 233); or (c) both. Since all fluxes are normal prior to 5 UT on Day 233, at least two hours after initiation of the Dst event, all possibilities (a), (b) and/or (c) involve a substantial time delay of 2-6 hours. In no case have we found the flux decrease to preceed the Dst decrease. The sequence of events can possibly be further clarified and the time delay sharpened if other satellite data in the MLT vicinity were available. Nevertheless, this is an example that indicate time delay in the initiation of outer belt relativistic electron decreases with Dst responses. At the same time, it must be emphasized that Dst and flux decreases are well correlated to a high degree on an event-by-event basis, as is shown in Figure 2. In other words, we have co-incidence but not necessarily co-initiation between the relativistic electron and Dst events. Vertical time markers, provided in Figure 2, give us the impression that on the coarse time scale the minima of Dst and relativistic electron events line up much better than the initiation points.

In the foregoing, we observe that the outer belt relativistic electrons have at least two distinct response times: an intermediate term response of tens of days and a short term response of a day or two. The revelation of these two time scales is not entirely new since previous work have reported on such response time scales. The CRRES/SEP data yield additional dynamical information available in the electron distribution functions which may help illucidate the nature of the short term responses.

The most important feature of our data is the ability to measure the distribution function. The short term response distribution functions of the relativistic electrons in the outer belt (L ~4–6.5) reveal a number of interesting features. They are:

(1) As is shown in Figures 3, 4, and 5, the shapes of the distributon functions remain relatively unchanged even though the total flux can change by some 3 orders of magnitude. These distribution functions are not different in shape from the normal outer belt distributions, the changes during the event are in flux level only. Relatively few pitch angle distribution functions during the short term responses were found to be peaked off zero

degrees in pitch angle ("butterflies").

(2) In the relativistic electron range, the energy spectral shape is also relatively unchanged throughout the short response duration.

(3) The relativistic electron flux levels before and after the short term response are also little changed; certainly there is little indication of before-after flux differences comparable to the total response itself.

(4) The features above, i.e. features (1), (2) and (3), are found in relativistic electrons throughout the outer belt (L $\sim$ 4–6.5).

(5) We do not find a local time preference for occurrence.

In order to recapitulate the above features that we have extracted from examination of a spectrum of events and to motivate our theoretical discussions that may lead to modeling these short term responses, we present in Figure 6, on panels A-I with orbital geometries, a space-time matrix of distribution functions, showing an event with the "typical" features that we have summarized from examination of a spectrum of events. In Figure 6, the time resolution is de-emphasized in order to encapsulate the sequential development of the distribution function as one goes through the event from pre-event (top row), through event development (middle row), to partial recovery (bottom row). The orbit locations and Dst values corresponding to the alphabetized sequence of distribution functions are shown on the orbit configuration figure for each row. This figure shows clearly that the pre-event flux gradient from L=5 outwards is deepened to an extent not explainable by bulk inward transport. [We are indebted to Dr. Mike Schulz for this observation.]

## DISCUSSION AND CONCLUSION

This repeatable orderly "dissolution–recovery" cycle of the outer belt short-term response, preserving roughly the shapes of pitch angle distributions and energy spectrum throughout a flux change that can be as much as three orders of magnitude, certainly requires some interpretive consideration. The features noted above are probably easy to explain when taken one at a time independently and without regard to each other. For example, the disappearance and subsequent recovery of flux from a given location, by itself, is easy to explain by simply assuming that the population is "transported in bulk with the field line to a different location". However, if one were to write a theory with such bulk dynamic transport properties in configuration space, the electric field response to the magnetic field changes, required by the transport, would make it difficult not to drastically change the energy spectral shape and to cause drastic particle loss to the atmosphere (thus changing the pitch angle distribution) at the same time. If there are drastic losses to the atmosphere in the initiation, where do we find relativistic electrons to replenish the outer

belt to account for rapid recovery within a few drift periods? Note that any bulk transport outwards decreases the energy. Further, if the outer belt electrons were transported elsewhere in bulk then how is feature (4) to be reconciled? In other words, where were the relativistic electrons during the response, for they were not found in bulk in the outer belt region sampled by our data base in L $\sim$ 4–6.5?

Without denying the possibility of some bulk transport, we would like to focus on the key features of (1) deep flux decrease correlated with the Dst response, signifying the thinning of the magnetic field, (2) the rough "conservation" of energy spectral shape and (3) rapid recovery to pre-event flux level.

If we interpret these features as limiting characteristics of the transport processes in the six-dimensional phase space involved, then we may hypothesize a major increase in trapping volume in configuration space, but without much loss to the atmosphere. The rapid recovery in flux can be accomplished by a reversible process restoring the original trapping volume and accounting for the tendency to recover to the original flux level. For such rapid recovery to take place reversibly, the dynamical processes acting on the population are likely to be adiabatic. It must be carefully noted here that we address effects that operate on the population as an aggregate, as do the CRRES/SEP data. An individual electron may gain or loose energy as it moves in a changed trapping volume, but the energy spectrum represent features of the population.

If we assume adiabaticity, then we can combine the above observed features with consequences of first adiabatic invariant conservation [e.g. Nakada et al., 1965; Barfield et al., 1971] to yield the beginning of a model of the outer belt short-term relativistic electron responses. [For purposes of expositional economy, we shall use non-relativistic expressions below. Our conclusions are not substantially changed if we use proper relativistic expressions.] If the first adiabatic invariant $\mu = (E/B)sin^2\alpha$, where $(E, B, \alpha)$ are respectively energy, magnetic flux and pitch angle, is conserved as the population undergoes the short-term dynamical process, then we require that

$$D\mu(E, B, \alpha)/Ds = 0 \tag{1a}$$

where the symbol $D/Ds$ denotes derivative along the dynamical trajectory of the state in six-dimensional phase space of the population. In other words, the state moves along $s(E, B, \alpha)$ in such a way as to keep $\mu$ equal to its initial value. The distribution function of the population, $f(E, L, \alpha) = f(\mu, J, \Phi)$, where $J$ and $\Phi$ are second and third invariants, must obey Liouville's Theorem, which states that the phase space volume containing representative points of the population moves along $s$ in an incompressible manner

$$Df(p_i, q_i, t)/Dt = 0 \tag{1b}$$

where $(p_i, q_i)$ is the set of cannonical co-ordinates of the system including the invariant variables above. The implications of (1) are rather clear: as the system moves along the phase space trajectory $s$ constrained by (1a), the constraint induces a transformation on $f(\mu, J, \Phi)$, the density of representative points in phase space.

While there is possibly a denumerable infinity of solutions that can satisfy (1), the observed features of the CRRES/SEP data hint that we can perhaps consider a subset solution of (1) of the form

$$f(\mu, J, \Phi) = g(\mu)\, h(J, \Phi) \tag{2}$$

with the the function $h(J, \Phi)$ slowly varying over the short-term event. This subset of distributions functions has a special property: application of Liouville's Theorem [e.g. Chiu and Schulz, 1978] along $s$ causes the distribution function $f$ to undergo a similarity transformation because the conserved invariant $\mu$ is contained in a separable part of $f$. Because of the special form, once the function $g$ is determined initially, the transformation of $f$ as the event evolves is uniquely determined.

Let us now apply the dynamical similarity property of $g(\mu)$ as required by Liouville's Theorem to a specific form of $g$ that characterizes the initial flux. Here two important features of the observations must be noted: (a) the initial quiet-time energy spectrum of outer belt electron flux $F$ in the energy range considered here can be well fit by a power law, and (b) energy spectrum is relatively unchanged throughout the short-term event. We shall show that (b) is a consequence of (a) plus the similarity property due to first invariant conservation.

Consider a power law flux parameterized by

$$F_i \propto (E_0/E_i)^{\beta} \tag{3}$$

where the subscript $i$ indicates the initial state, $\beta$ is a spectral index usually in the range of 2-4 and $E_0 \sim 1$ Mev is a scaling constant, for outer-belt electrons in our energy range. Since the distribution function $f$ is related to the flux $F$ by $f = F/(2m_e E)$, this specification in the initial state applied to the form (2) determines

$$g(\mu) = (\mu_0/\mu)^{\beta+1} \tag{4}$$

which is exactly equivalent to (3) in the initial state $\mu = \mu_i$. However, the assumption of first invariant conservation and the similarity transformation induced upon $f$ throughout the dynamical evolution of the short-term event imply much more than the specific parameterization (3) in the initial state because $\mu$ remaining constant specifies the variations in

its constituent parameters $(E, B, \alpha)$ as the population evolves through the event provided that $h$ is considered slowly varying on the short-term time scale.

First, from (4) and the invariance of $\mu$, the power law energy spectrum of this simple model is observed to remain the same power law throughout the event because $\mu$ is invariant throughout the event also, as we approximately noted in the observations. This notion is not new, since the invariance of power law spectrum under first invariant conservation was first noted by Nakada et al. [1965], who rejected the power law spectrum for protons precisely because this invariance property does not agree with inward diffusion to create the proton belt with an exponential spectrum. Here we invoke this property for a very different dynamical phenomenon governing outer belt electrons.

Second, as the Dst undergoes a decrease and recovery, so does the magnetic flux B in the L=4–6.5 region; therefore, (4) implies that the distribution function $f$ would undergo a decrease and recovery according to $B^{\beta+1}$. Since $\beta \sim 2-4$, the ring-current reduction of the outer belt magnetic flux, which is inversely equivalent to trapping volume in configuration space, leads automatically in this model to a drastic reduction of the distribution function, as observed. For example, a factor of 2 decrease in local $B$ leads to a factor of 8–32 reduction in flux. A corollary to this point is that the trapping volume increase predicted by our modeling hypothesis co-incides precisely with the outer portion of the outer belt. This can be seen from any generic magnetic field model expressed as the sum of the main field $B_0(r)$ plus the ring current field $\Delta B(r)$in this region

$$B(r) = B_0(r) - \Delta B(r) = B_0(r) - P(r) \times Dst \tag{5}$$

where $P(r)$ is a positive profile function which is constant at small L values, maximizing at L$\sim$4, vanishing at L$\gg$6.5. Thus, the effect of the magnetic disturbance and the trapping volume change is uniquely localized to the outer belt because of the dominance of $B_0$ at L$\leq$4 and the behavior of $P(r)$ at L$\geq$6.5.

Third, if the short-term dynamical processes remain adiabatic, the recovery to the initial state is necessarily implied, i.e. the state trajectory $s$ in phase space is a closed curve; thus resulting in relatively little difference in flux between the initial and the final states, as noted in the observations.

We seek in the above to develop a simple model that can account for some observed generalities of the short-term responses of the relativistic electron population in the outer belt. At this point, we do not seek quantitative accuracy, as we are in the process of compiling a data base of the short-term response events for quantitative modeling. This brief report summarizes the salient features of the observations and the modeling approach; therefore, it is also appropriate to outline the caveats and the relationship between the

short-term and intermediate-term responses, which were the previous focus in this project [Chiu et al., 1988; 1990].

(i) The focus of discussion in this report is the short-term response. Some properties of intermediate-term responses were touched upon, but no clear boundary line between the two classes has been developed. Clearly, there is a spectrum of Dst strengths and boundary lines, if any exist, will not be sharp. In this regard, we note in Figure 1 that outer belt electrons in the energy range treated here do not exhibit prolonged response behavior, as comparison of fluxes before and after the historic March 1991 event on the figure will show. The "adiabatic" features discussed here are not found in this major storm period.

(ii) The similarity evolution of the function $g(\mu)$ has implications on the pitch angle distribution as much as it has on energy spectrum and flux density. A power law in $sin\,\alpha$ is often invoked as model pitch angle distributions, as (4) would imply. However, it must be remembered that the second invariant is also a key function insofar as the pitch angle distribution is concerned. Further, during the deepest part of flux decreases, there are often not enough counts to determine an accurate pitch angle distribution; thus, we are unsure of the relative contributions of the functions $g(\mu)$ and $h(J,\Phi)$. Our previous work on simultaneous pitch angle and radial diffusion in the outer belt [Chiu et al., 1988,1990] will likely be able to give a model of the pitch angle distribution for the intermediate- term contribution to $h(J,\Phi)$ since applications were made to similar data with good results.

(iii) We have invoked the properties of first invariant conservation on the population as an aggregate to obtain our results. It must be noted that we have not imposed any mechanism on individual electron encounters with the geomagnetic field and field structures except in the case of trapping volume increase by intensification of the ring current. Until we examine the quantitative relationship between the pre-event spectral index and the amount of flux decrease in our data base, we must be careful in separating the consequences of first invariant conservation from the consequences of the ring current. There may be many dynamical processes that also conserve the first invariant, e. g. elastic scattering between relativistic electrons and magnetic structures, which are not necessarily directly controlled by the ring current. First invariant conservation is a more general dynamical concept than the specific way the magnetic field is decreased or the trapping volume is increased. It can turn out that we may need more than one first invariant conserving process to account for the severe flux decrease. Equivalently, a linear superposition of functions of the type (2) remains a solution of (1).

(iv) For recovery to take place within drift time scales, the relativistic electrons must be contained within the magnetosphere, implying insubstantial loss of outer-belt relativis-

tic electrons either to the atmosphere or to the heliosphere over the duration of the short term response. The magnetic gradient at the magnetopause may or may not be able to confine the dispersed relativistic electrons during the response event. But, by whatever containment mechanism, one should not detect substantial relativistic electrons outside the magnetosphere coincident with the short-term responses, thus allowing the total relativistic electron number to be approximately "conserved" so that the recovered flux level is not substantially changed from the pre-event level. This is a prediction as result of our considerations.

(v) We show in the highly time-resolved consideration of the response sample in the previous section that there is no co-initiation of flux decreases with the Dst event. Therefore, a simple model such as (2) and (4) obviously does not address the time delay question, which also shows up in Figure 6. However, by invoking a simple concept of first invariant conservation, we hope to have organized the salient features of these responses into an approximately viable perspective.

ACKNOWLEDGMENT

This paper is supported by Air Force Phillips Laboratory/Geophysics contract F19628-90-C-0097. The authors are indebted to Drs. Bob Robinson and R. Nightingale for CRRES/SEP data analysis support and to Drs. M. Schulz, G. Mullen, S. Gussenhoven and A. Vampola for discussions.

REFERENCES


Baker, D.N., R.L. McPherron, T.E. Clayton and R.W. Klebesadel, Linear prediction filter analysis of relativistic electron properties at 6.6 $R_E$, J. Geophys. Res., 95, 15, 133, 1990.

Baker, D.N., P.R. Higbie, E.W. Hones, Jr., and R.D. Belian, High-resolution energetic particle measurements at 6.6 $R_E$, 3, Low-energy electron anisotropies and short-term substorm predictions, J. Geophys. Res., 83, 4863, 1978.

Barfield, J.N., L.J. Lanzerotti, C.G. Maclennan, G.A. Paulikas and M. Schulz, Quiet-time observation of a coherent compressional Pc-4 micropulsation at synchronous altitude, J. Geophys. Res. 76, 5252, 1971.

Brown W.L., L.J. Cahill, L.R. Davis, C.E. McIlwain, and C.S. Roberts, Acceleration of trapped particles during a magnetic storm on April 18, 1965, J. Geophys. Res. 73, 153, 1968.

Chiu, Y.T., R.W. Nightingale, and M.A. Rinaldi, Simultaneous radial and pitch angle diffusion in the outer electron radiation belt, J. Geophys. Res., 93, 2619, 1988.

Chiu, Y.T., M.A. Rinaldi, and R.W. Nightingale, Toward dynamic modeling of the outer electron radiation belt, J. Geophys. Res. 95, 12069, 1990.

Chiu, Y.T. and M. Schulz, Self-consistent particle and parallel electric field distributions in the magnetosphere-ionosphere auroral region, J. Geophys. Res., 83, 629, 1978.

Mullen, E.G. and M.S. Gussenhoven, Results of space experiments: CRRES, J. Spacecr. Rockets, in press, 1992.

Nakada, M.P., J.W. Dungey, and W.N. Hess, On the origin of outer-belt protons, 1, J. Geophys. Res., 70, 3529, 1965.

Nightingale, R.W., R.R. Vondrak, E.E. Gaines, W.L. Imhof, R.M. Robinson, S.J. Battel, D.A. Simpson and J.B. Reagan, The CRRES spectrometer for electrons and protons (ONR 307-3), J. Spacecr. Rockets, in press, 1992.

Reagan, J.B., R.W. Nightingale, E.E. Gaines, W.L. Imhof and E.G. Stassinopoulos, Outer zone energetic electron spectral measurements, J. Spacecr. Rockets, 18, 83, 1981.

Sibeck, D.G., R.W. McEntire, A.T.Y. Lui, R.E. Lopez, and S.M. Krimigis, Magnetic field drift shell splitting: Cuase of unusual dayside particle pitch angle distributions during storms and substorms, J. Geophys. Res., 92, 13,485, 1987.

West, H.I., Jr., R.M. Buck and G.T. Davidson, The dynamics of energetic electrons in the Earth's outer radiation belt during 1983 as observed by the Lawrence Livermore National Laboratory's spectrometer by OGO 5, J. Geophys. Res., 86, 2111, 1981.

Figure Captions

Figure 1. Flux of relativistic electrons in the 759.5±206.5 keV energy channel integrated over all pitch angles and over the nominal L-value range 5.5–6.5 for the period of 1991 indicated on the bottom panel, which also shows the daily-averaged Kp index.

Figure 2. Fluxes of electrons in the 759.5±206.5 keV and 1156±206.5 keV channels in the L-range 4.5–6.5, shown correlated with the Dst index for the latter part of 1990.

Figure 3. Pitch angle distributions of the 759.5±206.5 keV electron channel as CRRES goes through locations A–F as CRRES visits the apogee on Orbit 66 on Day 233 of 1990 as indicated on the orbit geometry panel. The alphabetic CRRES locations and the corresponding Dst indices and times are shown on the right.

Figure 4. Same as Figure 3 except it is for Orbit 67 on Day 234 of 1990.

Figure 5. Same as Figure 3 except it is for Orbit 68 on Day 234/235 of 1990.

Figure 6. A matrix of distributions functions for the short-term response event on Days 319-320, 1991. The alphabetic sequence corresponds to the orbit geometry and Dst development shown on the right of each row. Each row shows the spatial dependence at the given orbit and each column shows the temporal development from orbit to orbit at the indicated fix location.

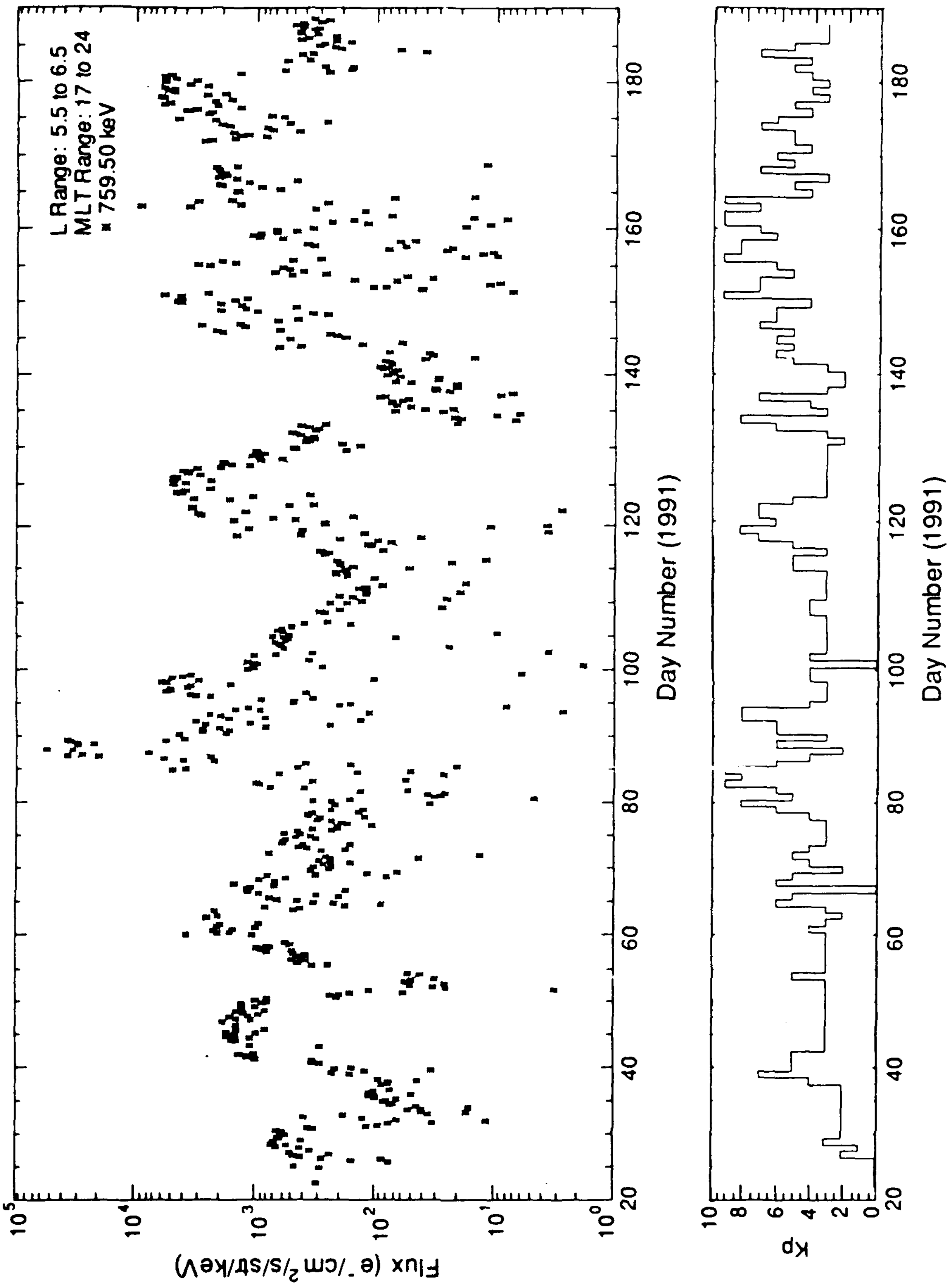

L Range: 5.5 to 6.5
MLT Range: 17 to 24
* 759.50 keV
Flux (e-/cm2/s/sr/keV)
Day Number (1991)
Kp
Day Number (1991)


Figure 1

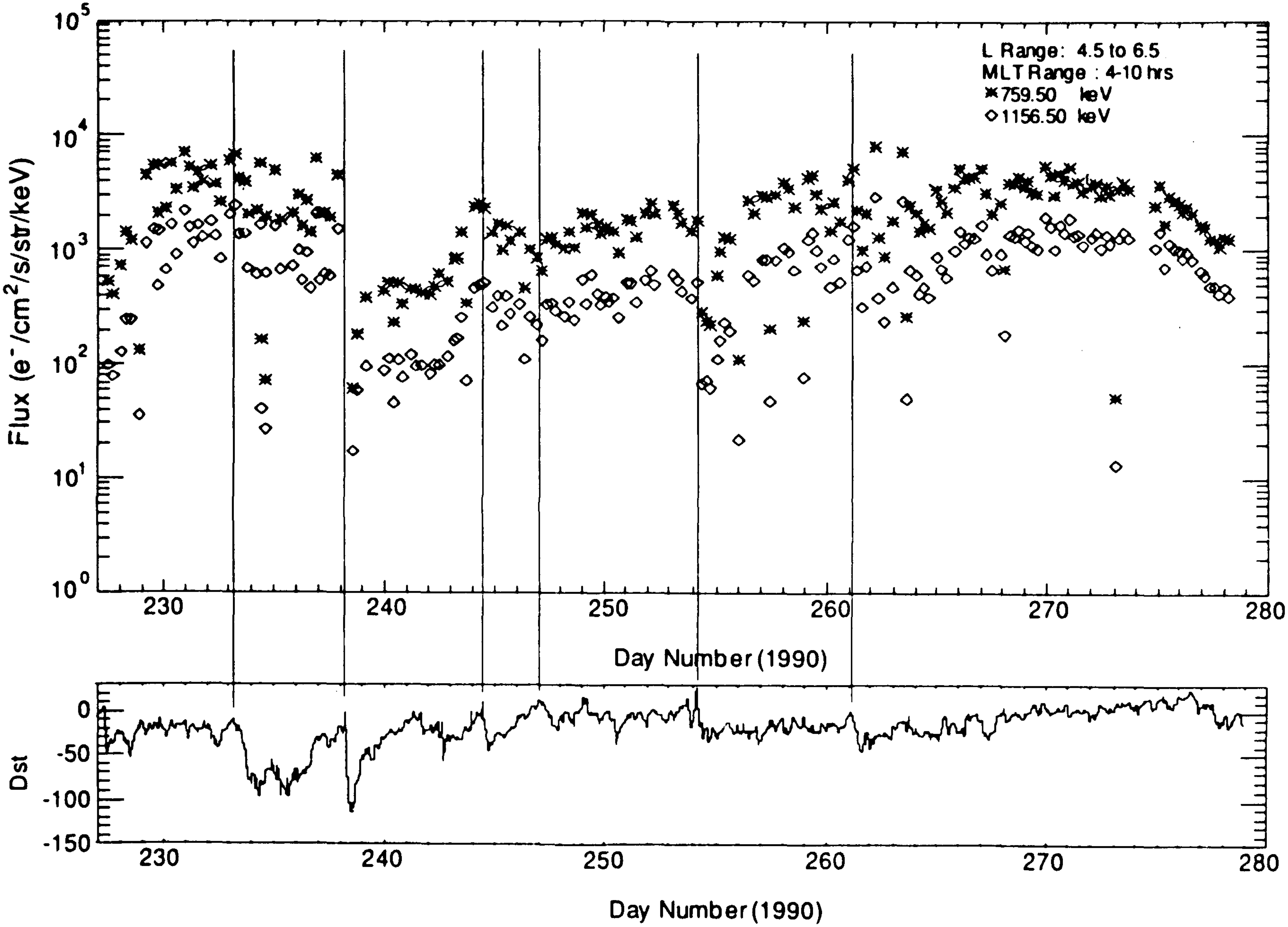
L Range: 4.5 to 6.5
MLT Range : 4-10 hrs
✱759.50 keV
◇1156.50 keV
Flux (e⁻/cm²/s/sr/keV)
Day Number (1990)
Dst
Day Number (1990)

Figure 2

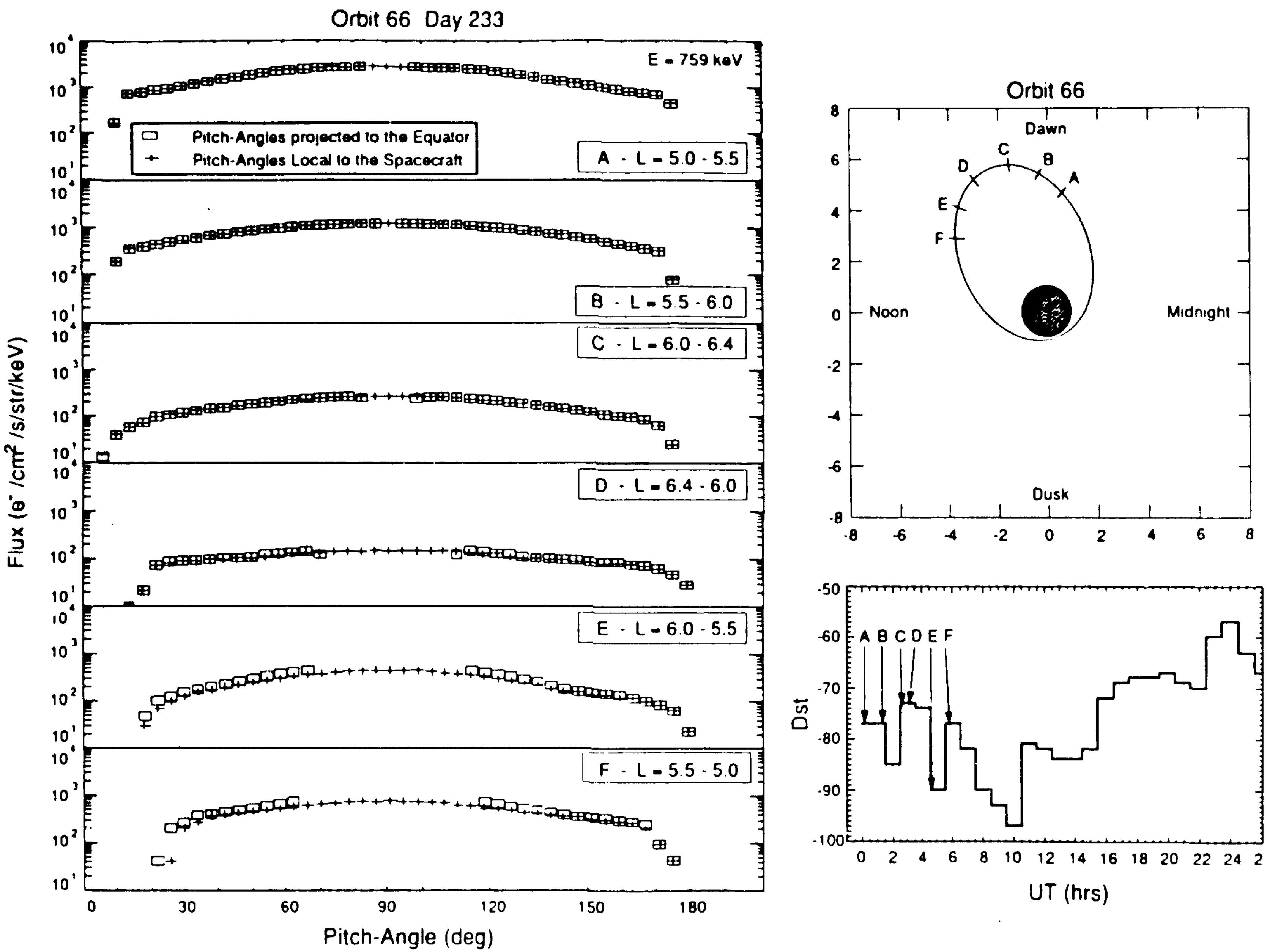

Orbit 66 Day 233
E = 759 keV
Pitch-Angles projected to the Equator
Pitch-Angles Local to the Spacecraft
A - L = 5.0 - 5.5
B - L = 5.5 - 6.0
C - L = 6.0 - 6.4
D - L = 6.4 - 6.0
E - L = 6.0 - 5.5
F - L = 5.5 - 5.0
Flux (e⁻ /cm² /s/str/keV)
Pitch-Angle (deg)
Orbit 66
Dawn
Noon
Midnight
Dusk
A B C D E F
Dst
UT (hrs)


Figure 3

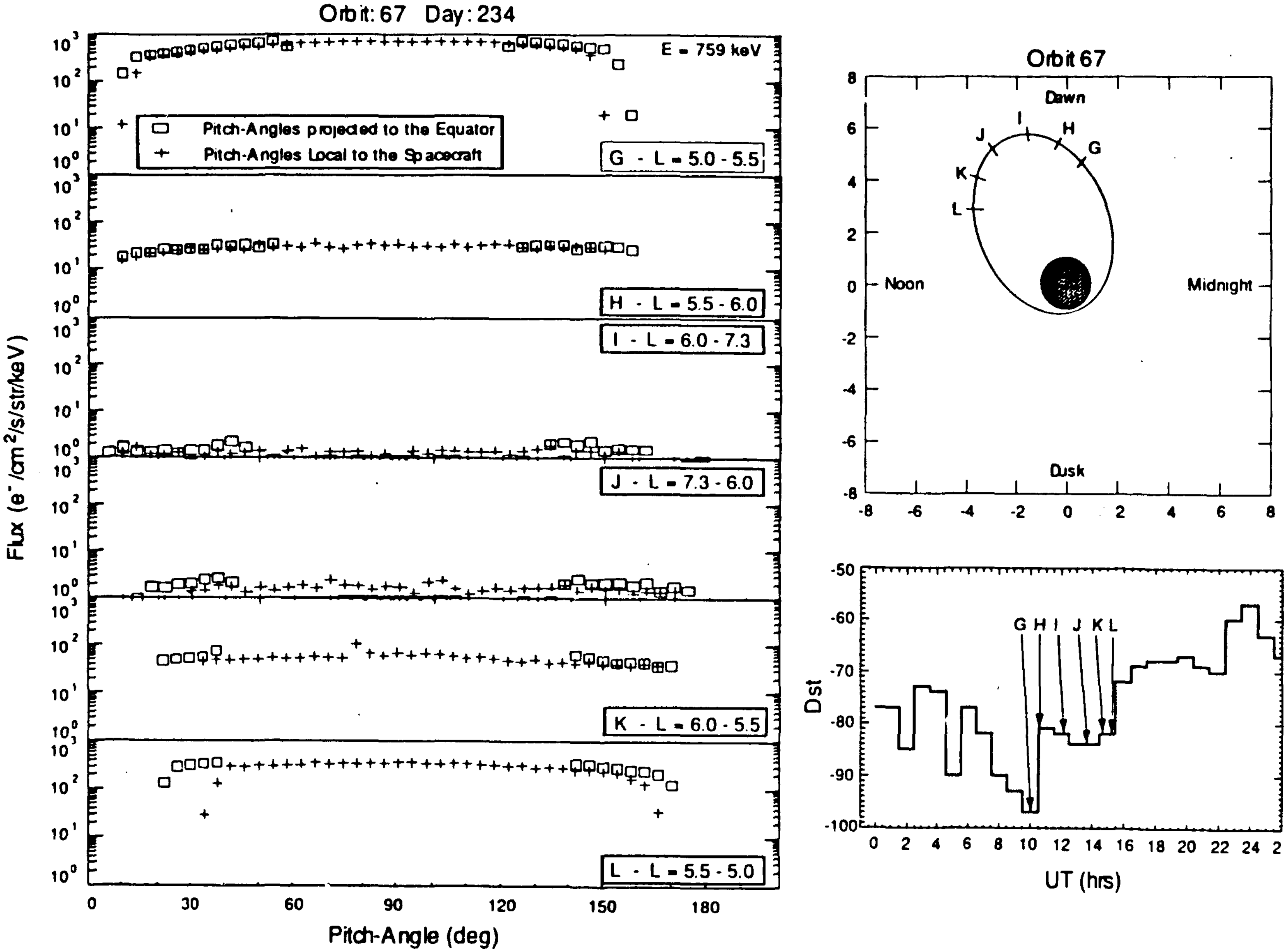

Orbit: 67 Day: 234
E = 759 keV
Pitch-Angles projected to the Equator
Pitch-Angles Local to the Spacecraft
G - L = 5.0 - 5.5
H - L = 5.5 - 6.0
I - L = 6.0 - 7.3
J - L = 7.3 - 6.0
K - L = 6.0 - 5.5
L - L = 5.5 - 5.0
Flux (e⁻/cm²/s/str/keV)
Pitch-Angle (deg)
Orbit 67
Dawn
Noon
Midnight
Dusk
G H I J K L
Dst
UT (hrs)


Figure 4

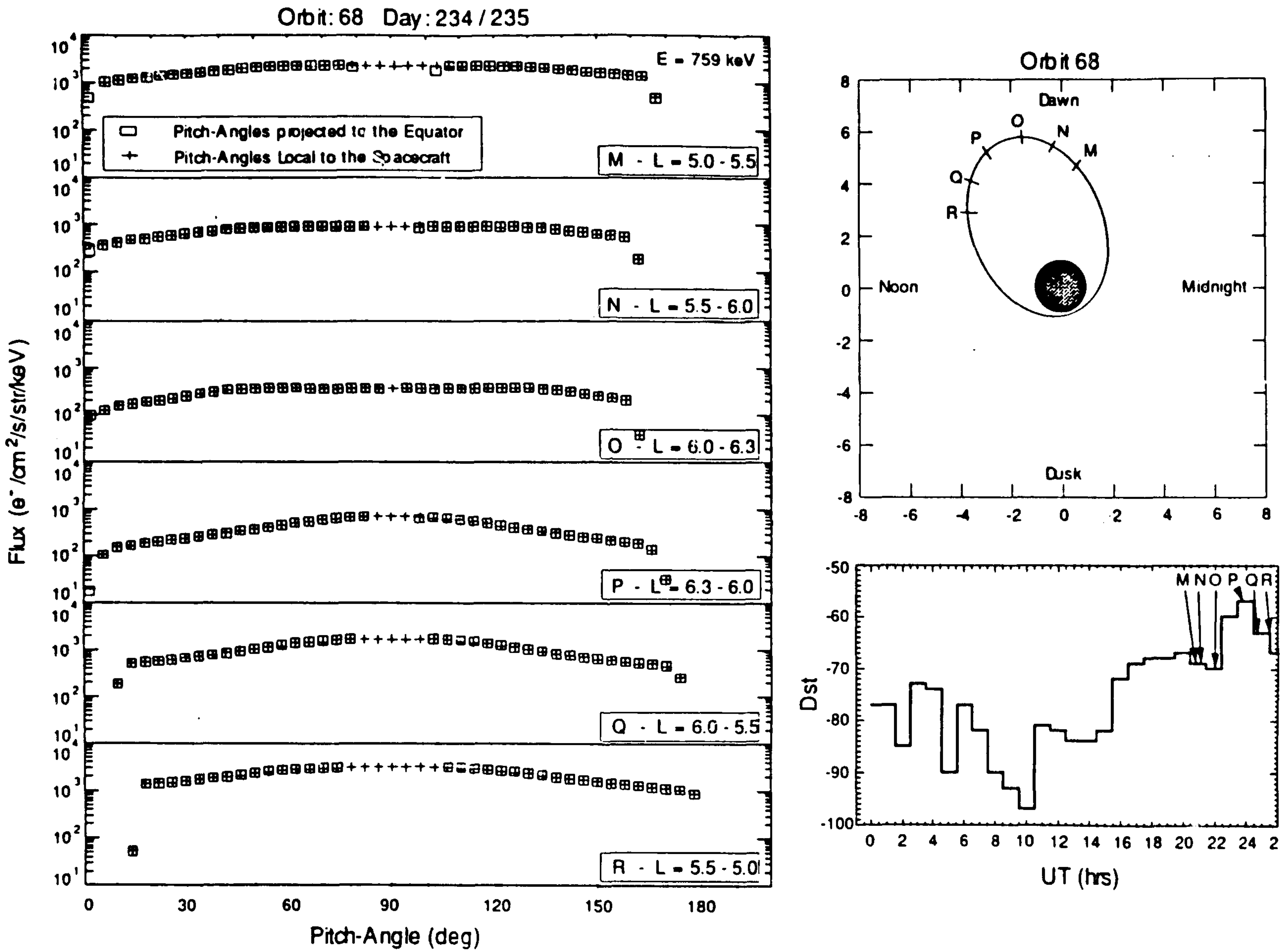

Orbit: 68 Day: 234 / 235
E = 759 keV
Pitch-Angles projected to the Equator
Pitch-Angles Local to the Spacecraft
M - L = 5.0 - 5.5
N - L = 5.5 - 6.0
O - L = 6.0 - 6.3
P - L = 6.3 - 6.0
Q - L = 6.0 - 5.5
R - L = 5.5 - 5.0
Flux (e⁻/cm²/s/str/keV)
Pitch-Angle (deg)
Orbit 68
Dawn
Noon
Midnight
Dusk
M N O P Q R
Dst
UT (hrs)


Figure 5

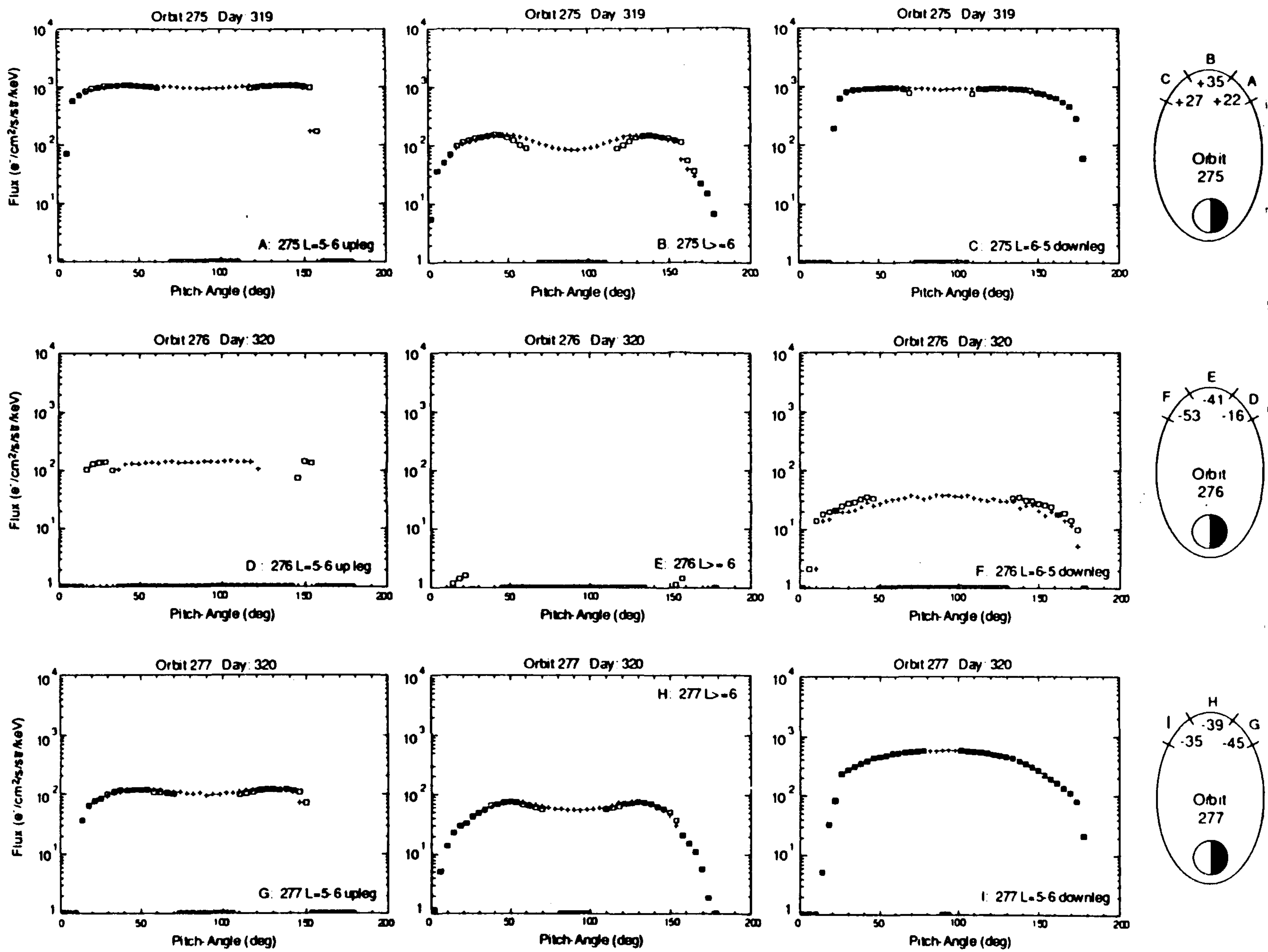

Orbit 275 Day 319
A: 275 L=5-6 upleg
B. 275 L>=6
C. 275 L=6-5 downleg
Orbit 276 Day 320
D: 276 L=5-6 up leg
E: 276 L>=6
F. 276 L=6-5 downleg
Orbit 277 Day 320
G: 277 L=5-6 upleg
H: 277 L>=6
I: 277 L=5-6 downleg
Flux (e⁻/cm²/s/sr/keV)
Pitch Angle (deg)
Orbit 275
+35 +27 +22
Orbit 276
-41 -53 -16
Orbit 277
-39 -35 -45


Figure 6

EXHIBIT 2

# SOURCE-SURFACE MODEL OF THE MAGNETOSHEATH

Y. T. Chiu and W. E. Francis

Lockheed Palo Alto Research Laboratory, Palo Alto, CA 94304

and

Michael Schulz

Space and Environmental Technology Center, The Aerospace Corp.

El Segundo, CA 90245

## Abstract

## 1. Introduction

The purpose of this work is to devise a reasonably simple and reasonably portable model for the draping of interplanetary magnetic field lines over and around the surface of the magnetosphere. The draping problem is ultimately magnetohydrodynamic (MHD) in structure, but simplifying approximations are generally regarded as acceptable. Thus, for example, Spreiter et al. [1966] have treated the problem as essentially hydrodynamic, such that magnetic field lines "go with the flow" that is obtained by solving the ordinary fluid equations (rather than the MHD equations) in the presence of a rigid obstacle shaped like the magnetopause. The approach used by Spreiter et al. [1966] is reminiscent of that invoked by Parker [1958] for modeling the interplanetary magnetic field in the absence of such an obstacle, and it appears to have been equally successful. Indeed, this approach forms the basis for the widely used magnetosheath model of Spreiter and Stahara [1980] and for various improvements upon that model, which Spreiter and Stahara have generously made available to the magnetospheric community.

The model of Spreiter and Stahara [1980] entails a numerical solution of the fluid equations over an appropriately chosen numerical grid. Even so, its results can be generated quite rapidly on a modern high-speed computer. Thus, the need for any significant improvement upon the Spreiter-Stahara model (except for replacement of the fluid equations by the MHD equations, which can best be done by the original authors) is open to question. Our rationale for the present work is that novel approaches to the solution of a previously treated geophysical problem often lead to unanticipated benefits and insights. Part of the basic idea of the present work is that it may be advantageous to derive the magnetic field (and eventually perhaps the flow-velocity field as well) in the magnetosheath from a superposition of analytical functions of the spatial coordinates.

END OF EXHIBIT 2